Rare genetic interstitial lung diseases: a pictorial essay

Raphael Borie [1,2], Laureline Berteloot [3,4], Caroline Kannengiesser [5], Matthias Griese [6], Aurelie Cazes[7], Bruno Crestani [1,2], Alice Hadchouel [8,9] and Marie Pierre Debray [10]

[1]Université Paris Cité, Inserm, PHERE, Paris, France. [2]Hôpital Bichat, APHP, Service de Pneumologie A, Centre constitutif du centre de référence des Maladies Pulmonaires Rares, FHU APOLLO, Paris, France. [3]Service d'Imagerie Pédiatrique, Hôpital universitaire Necker-Enfants malades, Paris, France. [4]INSERM U1163, Paris, France. [5]Laboratoire de Génétique, APHP, Hôpital Bichat, Paris, France. [6]Department of Pediatric Pneumology, Dr von Hauner Children's Hospital, Ludwig-Maximilians-University, German Center for Lung Research, Munich, Germany. [7]Département d'Anatomo-Pathologie, Hôpital Bichat, AP-HP, Paris, France. [8]AP-HP, Hôpital Universitaire Necker-Enfants Malades, Service de Pneumologie Pédiatrique, Centre de Référence pour les Maladies Respiratoires Rares de l'Enfant, Paris, France. [9]INSERM U1151, Institut Necker Enfants Malades, Université Paris Cité, Paris, France. [10]Service de Radiologie, Hopital Bichat, APHP, Université Paris Cité, Paris, France.

Corresponding author: Raphael Borie (raphael.borie@aphp.fr)

Shareable abstract (@ERSpublications)
The radiological pattern of genetically inherited interstitial lung diseases can provide clues suggestive of a specific genetic cause, in addition to extrapulmonary manifestations.
https://bit.ly/4cOZihp

Cite this article as: Borie R, Berteloot L, Kannengiesser C, *et al*. Rare genetic interstitial lung diseases: a pictorial essay. *Eur Respir Rev* 2024; 33: 240101 [DOI: 10.1183/16000617.0101-2024].

Received: 10 May 2024
Accepted: 22 Aug 2024

Abstract

The main monogenic causes of pulmonary fibrosis in adults are mutations in telomere-related genes. These mutations may be associated with extrapulmonary signs (hepatic, haematological and dermatological) and typically present radiologically as usual interstitial pneumonia or unclassifiable fibrosis. In children, the monogenic causes of pulmonary fibrosis are dominated by mutations in surfactant-related genes. These mutations are not associated with extrapulmonary signs and often manifest radiologically as unclassifiable fibrosis with cysts that can lead to chest wall deformities in adults. This review discusses these mutations, along with most of the monogenic causes of interstitial lung disease, including interferon-related genes, mutations in genes causing cystic lung disease, Hermansky–Pudlak syndrome, pulmonary alveolar proteinosis, lysinuric protein intolerance and lysosomal storage disorders, and their pulmonary and extrapulmonary manifestations.

Introduction

Genetic predisposition to pulmonary fibrosis has recently been the focus of American and European taskforces [1, 2]. Telomere-related gene (TRG) mutations are the most commonly identified mutations in families and the most frequently reported computed tomography (CT) scan pattern is that of usual interstitial pneumonia (UIP) [3]. In most families, no genetic cause is identified, suggesting polygenic risks that include common genetic variants such as rs35705950 *MUC5B* promoter gene polymorphism and environmental expositions. Interestingly, rs35705950 is particularly associated with an increased risk of a UIP pattern, both in idiopathic cases and in secondary contexts such as rheumatoid arthritis [4].

However, several other rare or ultrarare genetic mutations have been reported to cause interstitial lung disease (ILD), usually with a non-UIP pattern. These include mutations in surfactant-related genes (SRGs), interferon (IFN)-related genes and genes associated with cystic lung disease, Hermansky–Pudlak syndrome (HPS), pulmonary alveolar proteinosis (PAP), lysinuric protein intolerance, and lysosomal storage disorders. With a growing knowledge in this subject, in this pictorial essay we propose a focus on clinical and radiological presentations encountered in these rare diseases (tables 1, 2 and 3).

SRGs

Four surfactant proteins (surfactant (SP-)A, B, C and D) are secreted by alveolar epithelial cells. *ABCA3* and *NKX2-1* are also involved in the metabolism of surfactant proteins [5]. Homozygous *SFTPB* and

TABLE 1 Main genes causing inherited interstitial lung disease (ILD)

Main pattern	Pathway	Genes	Age at onset	Extrapulmonary phenotype
Fibrotic ILD	Surfactant	*SFTPA1/A2*	Adult	Brain–lung–thyroid syndrome only for *NKX2-1*
		SFTPB, *SFTPC*, *ABCA3*, *NKX2-1*	Newborn/ childhood	
Fibrotic ILD	Telomere	*TERT*, *TERC*, *RTEL1*, *PARN*, *NOP10*, *NHP2*, *ACD*, *NAF1*, *ZCCHC8*, *RPA*, *POT1*	Adult	Telomere biology disorder
		DKC1, *TINF2*	Childhood	
Fibrotic ILD	Lysosome-related mutations	*HPS-1*, *HPS-2*, *HPS-4*	Childhood and adult	Hermansky–Pudlak syndrome
		SMPD1	Childhood and young adult	Acid sphingomyelinase deficiency
Fibrotic ILD/diffuse alveolar haemorrhage	Interferon activation	*COPA*, *STING1*	Childhood and young adult	Lupus-like nephropathy and arthritis
Pulmonary alveolar proteinosis	GM-CSF signalling and monocyte macrophages activation	*CSF2RA*, *CSF2RB*, *GATA2*, *STAT5B*, *ADA1*, *ADA2*, *IRF8*, *SLC7A7*, *OAS1*, *CCR2*	Newborn and childhood	Immunodeficiency, cytopenias
	Cytosolic tRNA synthetases	*MARS1*, *YARS1*, *LARS1*, *AARS1*, *IARS1*, *FARS1*		Hepatomegaly
Cystic lung disease	mTOR activation	*TSC1*, *TSC2*	Adult	Tuberous sclerosis complex
	Tumour suppressors	*NF1*		Neurofibromatosis type 1
		FLCN		Birt–Hogg–Dubé syndrome
Pulmonary alveolar microlithiasis	Phosphate transport protein	*SLC34A2*	Adult	None

GM-CSF: granulocyte–macrophage colony-stimulating factor; mTOR: mammalian target of rapamycin.

TABLE 2 Main radiological signs and patterns

Genes	Pattern	Honeycomb	Cysts	GGOs	Other
SFTPA1/A2, ***SFTPB***, ***SFTPC***, ***ABCA3***, ***NKX2-1***	GGO±cysts +++ NSIP DIP	Rare	+ and emphysema-like lesions	++	Lung cancer, chest wall deformities (childhood onset)
TERT, ***TERC***, ***RTEL1***, ***PARN***, ***NOP10***, ***NHP2***, ***ACD***, ***NAF1***, ***ZCCHC8***, ***RPA***, ***POT1***, ***DKC1***, ***TINF2***	UIP ++ Unclassifiable fibrosis ++ (predominant upper-lung or centrilobular fibrosis, PPFE features) PPFE HP	+++	None	+ and subpleural consolidations	None
HPS-1, ***HPS-2***, ***HPS-4***	Unclassifiable fibrosis ++ UIP	+	None	+	None
SMPD1	GGO+septal thickening	None	Rare	+++ crazy paving	None
COPA, ***STING1***	DAH features	+	+	+++	Mediastinal adenomegalies
	Unclassifiable fibrosis	+	++	++	
CSF2RA, ***CSF2RB***	Typical PAP	+	None	+++ crazy paving	None
GATA2	Nodules+GGO+reticular+emphysema	None	None	++ crazy paving, consolidations	None
MARS1	PAP pattern evolving to lung fibrosis	++	None	None	None
TSC1, ***TSC2***	Predominant cystic pattern	None	+++	None	Nodules Pleural effusion
NF1		None	+++ and emphysema	+	
FLCN		None	++	None	
SLC34A2	GGO and nodular lung calcifications	None	None	None	Calcifications

+ to +++: possible to frequent presence; DAH: diffuse alveolar haemorrhage; DIP: desquamative interstitial pneumonia; GGO: ground-glass opacity; HP: hypersensitivity pneumonitis; NSIP: nonspecific interstitial pneumonia; PAP: pulmonary alveolar proteinosis; PPFE: pleuroparenchymal fibroelastosis; UIP: usual interstitial pneumonia.

TABLE 3 Main characteristics of the genetic syndromes associated with interstitial lung disease

Syndrome	Haematological involvement	Hepatic involvement	Skin involvement	Other nonpulmonary involvement
Brain–lung–thyroid syndrome	None	None	None	Hypothyroidism Chorea
Telomere biology disorder	Thrombocytopenia Macrocytosis myelodysplastic syndrome Acute leukaemia	Portal hypertension	Premature grey hair	Rare
Hermansky–Pudlak syndrome	Bleeding diathesis	None	Oculocutaneous albinism	Nystagmus
Acid sphingomyelinase deficiency	Thrombocytopenia	Hepatosplenomegaly	None	None
Interferonopathy	None	None	Mild rash or livedo to severe ulcerative lesions	Fever Lupus-like nephropathy Arthritis
Aminoacyl-tRNA synthetases	Anaemia	Elevated liver enzyme Hepatomegaly	None	Failure to thrive Neurological, muscular and vascular abnormalities
GATA2 deficiency	Monocytopenia Myelodysplastic syndrome Acute leukaemia	None	None	Nontuberculous mycobacteria infection
Tuberous sclerosis complex	None	Liver angiomyolipomas	Hypomelanotic macules Angiofibromas Ungual fibromas Shagreen patches	Structural brain lesions
Neurofibromatosis type 1	Rare	Rare	Café au lait macules Axillary or groin freckling	Neurofibroma Glioma Lisch nodules Bony dysplasia
Birt–Hogg–Dubé syndrome	None	None	Cutaneous fibrofolliculomas	Renal tumours

ABCA3 mutations have been associated with neonatal respiratory distress syndrome [6], whereas *SFTPD* mutations have not been associated with ILD. Homozygous *ABCA3* mutations can also be revealed in infants and children, and sometimes in adults [7]. Heterozygous *SFTPC* mutations are usually reported in childhood ILD but may also be discovered in young adults with ILDs [8–10]. *SFTPA1* and *SFTPA2* heterozygous mutations are almost exclusively associated with adult-onset ILD and with an increased risk of lung cancer. ILD related to heterozygous *NKX2-1* mutations may be associated with hypothyroidism, ILD and neurologic anomalies (*e.g.* hypotonia, developmental delay and chorea), known as brain–lung–thyroid syndrome [11], but may also be associated with isolated ILD in infants, children and adults [9–11]. More than 100 adult ILD patients with SRG mutations have been identified to date [8–10, 12, 13].

The CT pattern is frequently atypical for UIP for any SRG, including atypical distribution of fibrosis and ground-glass-predominant ILD, frequently associated with cysts. The clinical and radiological presentation of ILD in adults associated with homozygous *ABCA3* mutations and heterozygous *SFTPC* mutations may exhibit similarities in terms of diffuse ground-glass opacities, septal thickening and cysts of variable size (figure 1) [14, 15]. The cysts are often small in size and with a preferential scattered distribution in the upper lobes and sub-pleural areas. In addition, some scattered centrilobular emphysematous lesions may also be present. SRG mutation-related ILD may also show CT features evoking nonspecific interstitial pneumonia (NSIP), desquamative interstitial pneumonia (DIP), hypersensitivity pneumonitis or, very rarely, pleuroparenchymal fibroelastosis (PPFE) (figure 2) [16, 17]. Young adults with childhood-onset SRG-related ILD may present chest wall deformities, such as pectum excavatum, pectum carinatum, thoracic asymmetries and scoliosis. Due to the high risk of lung cancer associated with SRG mutations in adults, any change in CT features, including the appearance of consolidation, masses or nodules, should raise the question of a possible lung cancer [13, 17, 18].

An important feature of SRG-related ILD is the great heterogeneity in clinical presentation, particularly in age of onset and in CT pattern, even within the same family [19]. The most frequent diagnosis is unclassifiable fibrosis, but idiopathic pulmonary fibrosis (IPF), NSIP, organising pneumonia or DIP have

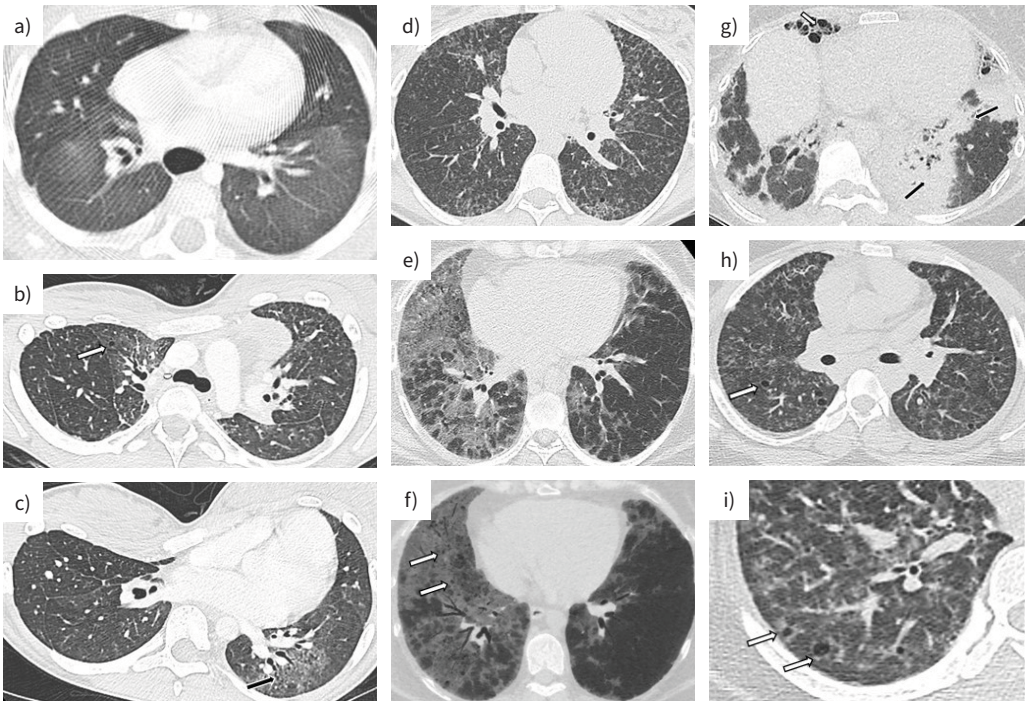

FIGURE 1 Computed tomography (CT) patterns associated with surfactant-related gene (SRG) mutation. a) Interstitial lung disease (ILD) revealed at the age of 8 months in 2003, in a *SFTPC* mutation carrier infant, showing diffuse ground-glass opacities. b) At the age of 14 years, the patient received prednisone and the chest CT performed in 2018 (b and c) shows less extensive ground-glass opacities, but mild traction bronchiectasis (black arrow), mild subpleural reticular opacities and small cysts (white arrow) have appeared. A severe thoracic deformation (pectum excavatum and scoliosis) has developed. d) 32-year-old smoking woman with an *SFTPA1* mutation presenting with predominantly ground-glass ILD, accompanied by reticular and small nodular opacities, which remained stable for several years following smoking cessation. e) 30-year-old nonsmoking woman with mostly ground-glass opacities associated with a compound heterozygous *ABCA3* mutation and associating small cysts (f white arrows), best depicted using minimum intensity projection reconstruction. g) 47-year-old smoking woman with known fibrosing ILD (honeycombing, white arrow) associated with *NKX2-1* mutation and newly appeared consolidations (black arrows) that were eventually related to lung cancer. h and i) 14-year-old girl with *SFTPC* mutation with ground glass and reticular opacities and associated small cysts (white arrows).

also been reported [15]. The association of cystic or centrilobular emphysematous scattered lesions is one of the hallmarks of SRG-related ILD and should raise suspicion for this diagnosis.

In children, successful immunomodulatory treatments, including prednisone, azithromycin and hydroxychloroquine, have been reported in case reports and short series [5, 20–22]. In adults, a recent series of 23 patients with SRG mutation-related ILD showed a comparable decline of forced vital capacity (FVC) and survival between SRG mutation carriers and IPF, leading to possible indication for antifibrotic drugs and lung transplantation in these patients [23, 24].

Telomere biology disorders

The telomere region is located at the ends of chromosomes and requires telomerase activity to slow down the shortening of telomere length [25]. 14 TRGs, namely *TERT*, *TERC*, *RTEL1*, *PARN*, *DKC1*, *TINF2*, *NOP10*, *NHP2*, *ACD*, *NAF1*, *ZCCHC8*, *RPA1*, *RPA2* and *POT1*, have been reported to cause ILD, most with autosomal dominant transmission. TRG mutations are the most common mutations identified in ILD patients, with heterozygous TRG mutations detected in 25–35% of the familial forms of pulmonary fibrosis (FPF) cases involving *TERT* (≈15%), *RTEL1* (5–10%), *PARN* (≈5%) and *TERC* (≈3%) [26–36]. TRG mutations have primarily been linked with telomere biology disorders in children and neonates such as dyskeratosis congenita, including mucocutaneous, haematological and liver abnormalities, and rare nonpulmonary diseases [37]. ILD in TRG mutation carriers is diagnosed at a mean age of 60 years [3, 27]

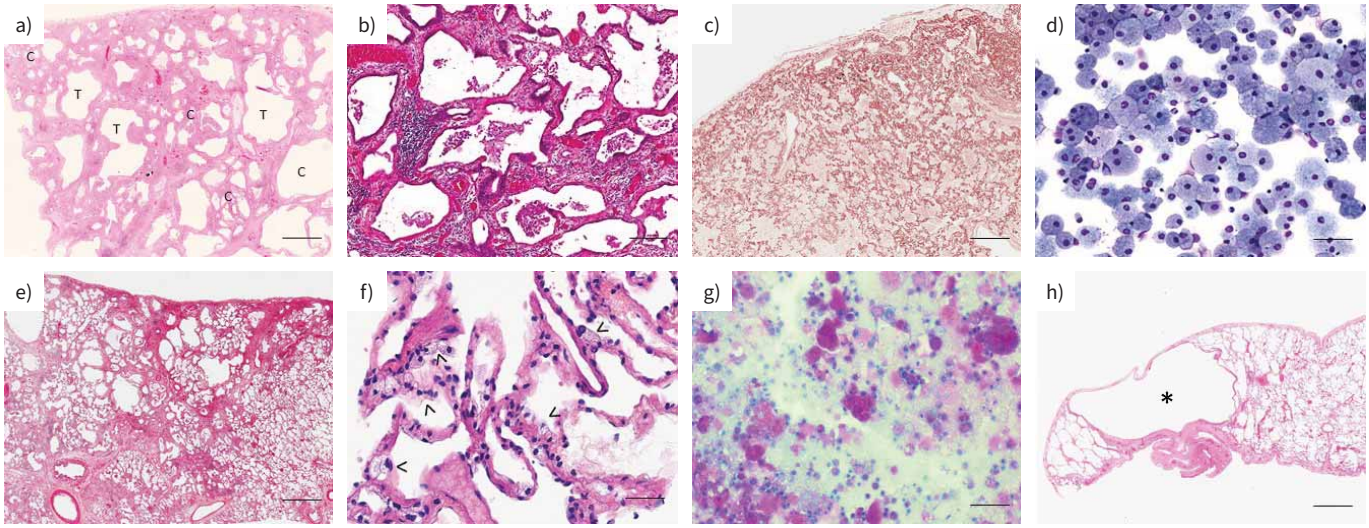

FIGURE 2 Representative pathology of the lung in rare genetic interstitial lung diseases. a) 33-year-old man with an interstitial lung disease (ILD) related to an *SFTPC* mutation. Explanted lung displayed fibrosis with numerous traction bronchiectasis (T) and honeycomb cysts (C). Pathological pattern was indeterminate for usual interstitial pneumonia (UIP) (haematoxylin–eosin–saffron (HES); bar: 1 mm). b) 34-year-old woman with an ILD related to an *SFTPA1* mutation (HES; bar: 200 µm). Focal pattern of mixed cellular and fibrotic nonspecific interstitial pneumonia with bronchiolar metaplasia on a surgical lung biopsy in an otherwise unclassifiable ILD. c) 66-year-old woman with an ILD related to a *TERT* mutation. A pleuroparenchymal fibroelastosis pattern was diagnosed on the explanted lungs (orcein; bar: 1 mm). d) Bronchoalveolar lavage fluid (BALF) from an acid sphingomyelinase deficiency-B patient. Numerous large foamy macrophages on May–Grünwald–Giemsa staining (bar: 100 µm). e) 36-year-old man with an ILD related to Hermansky–Pudlak syndrome (HPS) mutation. Explanted lungs displayed a "probable UIP" pattern (HES; bar: 1 mm). f) 51-year-old woman with an ILD related to HPS mutation (same patient as figure 3g). Clear and vacuolated type II pneumocytes (>) were observed on transbronchial biopsy (HES; bar: 50 µm). g) Periodic acid Schiff staining (PAS) of BALF from a 15-month-old boy with pulmonary alveolar proteinosis related to *MARS1* mutations. PAS+ macrophages associated with extracellular PAS+ material (bar: 100 µm). h) 49-year-old woman with asymptomatic cystic lung disease revealing Birt–Hogg–Dubé syndrome (same patient as figure 7k). Surgical lung biopsy revealed cysts (*) along the pleura and bronchovascular bundles (HES; bar: 1 mm). Images courtesy of Philippe Drabent and Alice Guyard (Department of Pathology, Hospital Necker and Bichat, APHP, Paris, France).

and is associated with extrapulmonary manifestations, such as thrombocytopenia and abnormal liver enzymes, in only 8–54% of cases [38].

A radiological UIP pattern is reported in 46–74% of ILD patients (figure 3) [3, 27, 29]. Unusual signs are reported in 13–20% of cases, including PPFE and upper-lung or centrilobular-predominant fibrosis [3, 27, 29]. The most commonly reported ILD diagnoses include IPF (45–47%), unclassifiable fibrosis (19–30%), fibrotic hypersensitivity pneumonitis (7–11%) and PPFE (5–10%) (figure 2) [3, 27, 29]. A normal chest CT scan associated with hypoxaemia should raise the suspicion of hepatopulmonary syndrome in a TRG mutation carrier patient [39].

Compared to patients without TRG mutations, patients with ILD and TRG mutations have been reported to have a more rapid decline in FVC (210–300 mL·year^{-1}), regardless of the TRG involved and the ILD diagnosis, leading to respiratory failure, lung transplant or death [27, 40, 41].

Lysosome-related mutations

Among lysosomal-related diseases, two genetic conditions may be revealed by an ILD, namely acid sphingomyelinase deficiency (ASMD), which is a historical lipid storage disorder, and HPS.

ASMD, Niemann–Pick disease and lysosomal storage disorders

ASMD is a lipid storage disorder caused by reduced activity of the lysosomal enzyme acid sphingomyelinase due to autosomal recessive transmission of an *SMPD1* gene variant. Loss of function results in sphingomyelin accumulation in the central nervous system, spleen, liver and lungs. The prevalence of ASMD is 1:50 000–1:250 000. Previously known as Niemann–Pick type A, infantile neurovisceral ASMD is fatal in early childhood. ASMD-B should be suspected in patients with ILD, splenomegaly, thrombocytopenia or low high-density lipoprotein cholesterol. Up to a third of patients

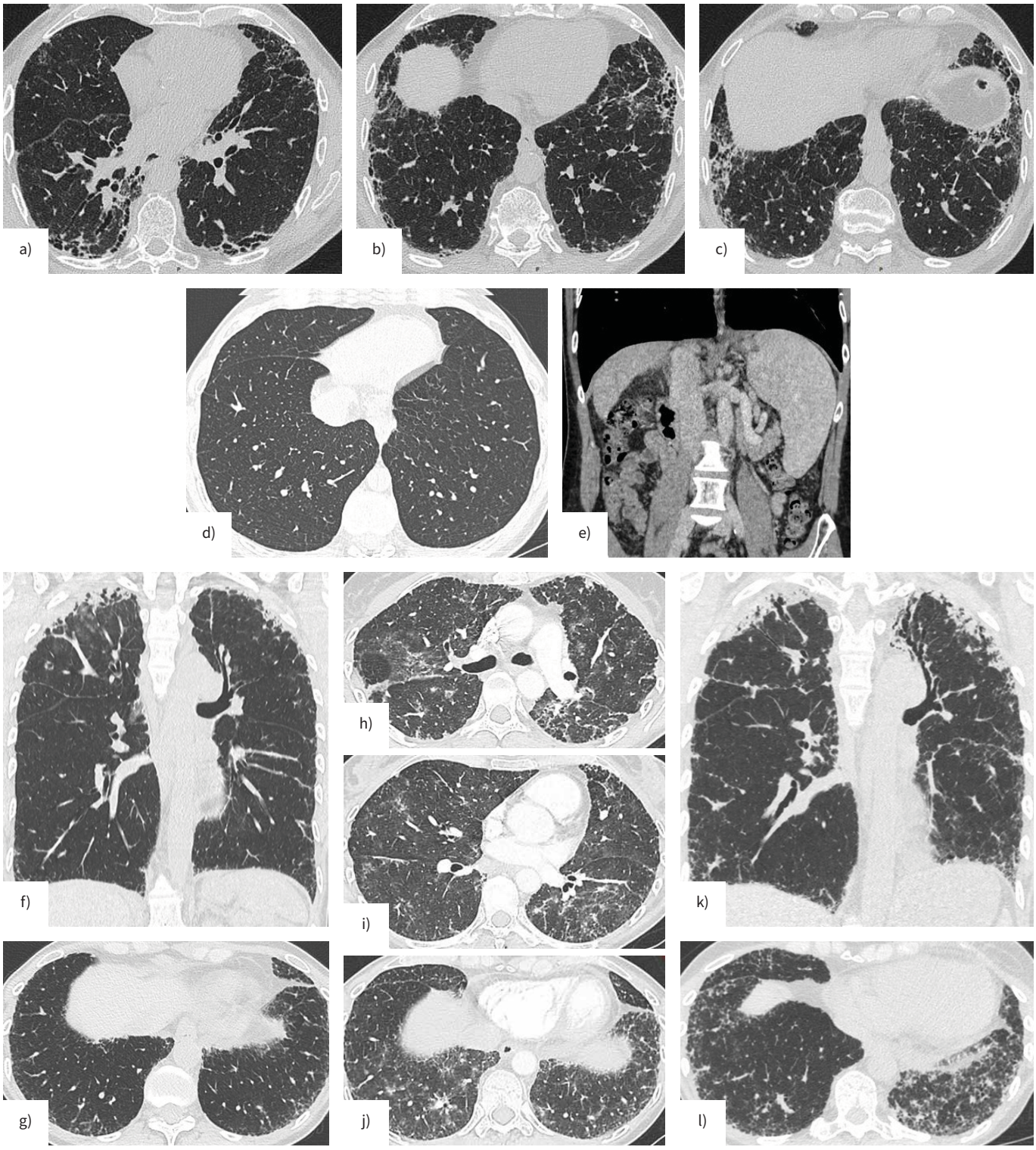

FIGURE 3 Computed tomography (CT) patterns associated with telomere-related gene mutation. a, b and c) Usual interstitial pneumonia pattern (UIP) in a 67-year-old *TERT* mutation carrier. d and e) Hepatopulmonary syndrome in his 34-year-old *TERT* mutation carrier son without interstitial lung disease, related to liver cirrhosis (e) splenomegaly and signs of portocaval collateral veins). f) CT scan suggestive of pleuroparenchymal fibroelastosis (PPFE) in a 47-year-old nonsmoking *TERC* mutation carrier with associated mild subpleural reticular opacities in the lower lobes (g). h, i and j) Acute respiratory failure a few months after diagnosis related to *Pneumocystis jirovecii* infection with initial improvement but evolving to progressive pulmonary fibrosis, involving both the subpleural apical consolidations related to PPFE 5 years later and the lower reticular opacities, indeterminate for UIP (k and l).

show a cherry-red macula without other signs of neurological or ophthalmological disease [42]. Adrenal gland calcifications and enlargement have also been reported [43].

Up to 90% of ASMD-B patients present with ILD [44], which is usually detected in children or young adults. The most frequent signs are ground-glass opacities (≈100%), interlobular septal thickening (≈100%) and intralobular lines (90–100%). Superimposed ground-glass opacities and reticulation, seen in up to 40% of cases, may be reported as a "crazy-paving" pattern (figure 4) [44, 45]. Other rare radiological signs have been reported, such as calcified pulmonary nodules cysts, centrilobular nodular opacities, peribronchovascular thickening, atelectasis, bronchiectasis and emphysema [44, 45]. Radiological abnormalities are bilateral and symmetric with a basal predominance [45]. Splenomegaly is always present, whereas the presence of hepatomegaly, splenic nodule and adrenal gland enlargement, and calcifications is variable.

When performed, bronchoalveolar lavage (BAL) shows "sea-blue" histiocytes or Niemann–Pick cells, confirming the diagnosis (figure 2) [46]. Although a lung biopsy is not typically required for diagnosis, which is made by enzyme activity and *SMPD1* sequencing, histopathologic findings of interstitial fibrosis without significant architectural distortion have been reported.

There is a no correlation between the extent of ILD on CT and functional impairment. Prognosis used to be determined by the presence of hepatosplenomegaly with secondary thrombocytopenia and ILD.

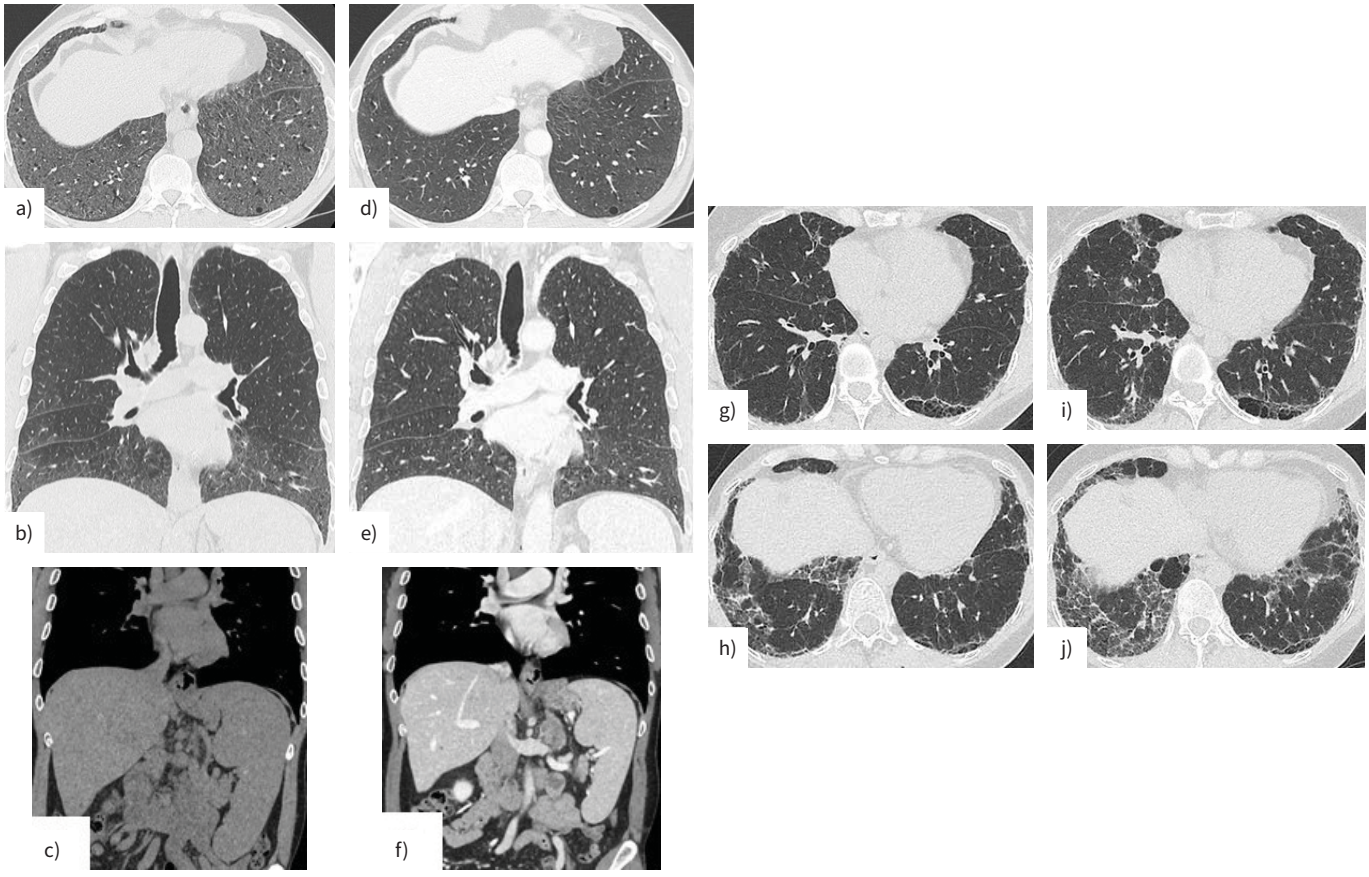

FIGURE 4 Computed tomography (CT) patterns associated with acid sphingomyelinase deficiency (ASMD) and Hermansky–Pudlack syndrome. a, b and c) 58-year-old man with interstitial lung disease (ILD) and splenomegaly secondary to ASMD. The chest CT shows basal predominant ground-glass opacities with limited superimposed septal lines in addition to a large splenomegaly and mild hepatomegaly. After 1 year with olipudase therapy, the ILD dramatically improved (d and e) and the volume of both spleen and liver decreased (f). This correlated with the pulmonary function test results and symptoms. g, h) The diagnosis of Hermansky–Pudlak syndrome with ILD was established in a 51-year-old woman presenting with a history of spontaneous bleeding and albinism. Chest CT scan, indeterminate for usual interstitial pneumonia, showed subpleural predominant reticular and ground-glass opacities, with some peribronchovascular distributed opacities. Honeycombing was also present. i, j) After 2 years follow-up, the patient exhibited clinical functional and radiological progression of pulmonary fibrosis but has so far declined any antifibrotic therapy.

However, recent advancements in enzyme replacement therapy with olipudase alfa have shown dramatic improvements in both splenomegaly and ILD in a phase 3 trial [47].

Gaucher's disease is an autosomal recessive disease caused by glucocerebrosidase mutations [48]. Gaucher's disease is characterised by bone disease, such as osteopenia, focal lytic or sclerotic lesions, and osteonecrosis, hepatosplenomegaly, thrombocytopenia, anaemia, pulmonary disease and central nervous system disease [48]. Since its introduction in 1991, enzyme replacement therapy has greatly altered the natural history of the disease [49]. Cases of ILD and death from pulmonary failure, which were commonly reported before 1991, have now become exceptional.

Fabry disease is an X-linked lysosomal storage disorder caused by *GLA* mutations [50]. The enzymatic defect leads to the progressive accumulation of glycosphingolipids, resulting in neurological, ocular, skin, renal and cardiac manifestations [50]. Respiratory symptoms are most frequently related to COPD-like or cardiac involvement. Respiratory symptoms are common, but ILD is exceptional.

HPS

Eight genes with autosomal recessive transmission have been reported to cause HPS with constant coagulation dysfunction and albinism. However, only three of these genes (*HPS-1*, *HPS-2* and *HPS-4*) are linked to ILD. HPS mutations lead to abnormal protein trafficking, affecting lysosome-related organelles [51]. About 100 HPS-ILD adult cases have been reported.

The most frequently reported radiological pattern is indeterminate for UIP (figure 4). Histology may show a UIP pattern, superimposed with hyperplastic alveolar epithelial cells filled with enlarged lamellar bodies and phospholipid-rich droplets (figure 2) [52].

Fibrosing lung disease in HPS begins in early childhood [53]. Individuals reaching adulthood with pulmonary fibrosis present respiratory failure and death occurring at a mean age of 37. The safety and efficacy of pirfenidone and nintedanib in this context remain unknown and these patients face additional risks during lung transplantation due to clotting dysfunction [54].

Interferonopathies

Autoinflammation is an evolving field with the identification of more than 50 new monogenic autoinflammatory diseases identified in the last 10 years [55]. *COPA* and *STING1* are two genes linked to IFN signalling and associated with ILD [56, 57].

IFN pathway activation can be detected by IFN activity assay, IFN transcriptomic signature or IFN dosage. These tests usually require specific samples (fresh frozen or PAXgene) and are not specific to *COPA* or *STING1* variants [58]. Genetic analysis is usually performed in cases of suggestive clinical or biological evidence.

STING (stimulator of IFN genes)-associated vasculopathy with onset in infancy (SAVI) syndrome

SAVI is an autosomal dominant disease caused by a gain-of-function variant in *STING1*, resulting in the activation of the STING, IFN and NF-κB pathways [59].

Since its initial description in 2014, more than 70 SAVI cases have been reported, with two more common variants [59]. Three-quarters of SAVI patients present pulmonary manifestations in adolescence or early adulthood, mainly ILD and, less commonly, diffuse alveolar haemorrhage (DAH) [59, 60].

SAVI patients may present with cerebrovascular, articular or renal involvement [59].

The CT scan may show asymmetrical features suggestive of DAH, such as ground-glass opacities. Additional findings may include septal thickening, consolidation, reticular opacities and cysts, as well as signs of fibrosis (traction bronchiectasis, volume loss and honeycombing) and mediastinal adenomegalies (figure 5) [61]. BAL may confirm DAH or show lymphocytic, neutrophilic or mixed predominance alveolitis [62]. Lung histology may show unclassifiable interstitial fibrosis in addition to possible B- and T-cell infiltration with lymphoid follicles or features suggestive of pulmonary vasculitis or DIP [59].

The efficacy of Janus kinase (JAK) inhibitors has been reported in SAVI patients, including after lung transplantation, but pulmonary fibrosis may progress and require lung transplantation [60].

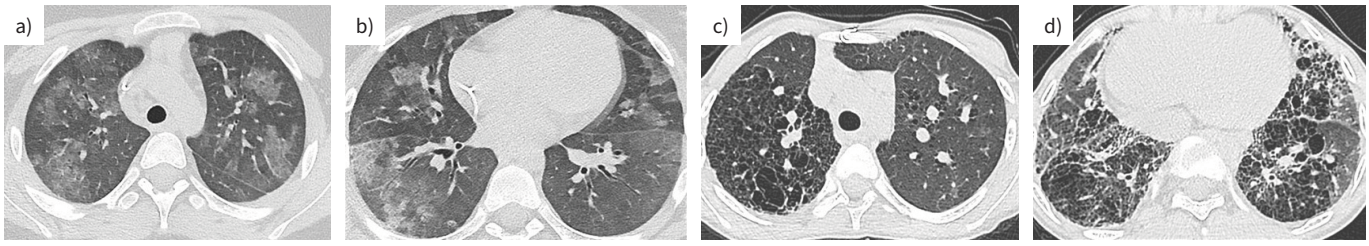

FIGURE 5 Computed tomography (CT) patterns associated with interferonopathies. a and b) CT scan of a 10-year-old girl with *COPA* syndrome showing bilateral ground-glass opacities with no specific area predilection. The opacities are sometimes confluent or associated with thickened interlobular septa and intralobular lines with a crazy paving appearance. Pattern suggestive of alveolar haemorrhage that led to the diagnosis of a *COPA* mutation. c and d) CT scan of a 14-year-old boy with *STING*-associated vasculopathy with onset in infancy showing a fibrosing interstitial lung in association with dry macular eruptions without loss of substance that led to the diagnosis of a *STING* mutation.

COPA

At least 10 missense variants have been identified in *COPA*, with around 60 patients reported to have heterozygous mutations in this gene [56, 63]. The penetrance can be up to 75% with 25% of asymptomatic adult carriers. Pathogenic *COPA* variants induce a strong activation of the IFN pathway [64].

The first flare usually occurs before the age of 5, although the initial flare may also occur in adulthood. Extrapulmonary manifestations usually include arthritis (75%) and lupus-like nephropathy (50%) that may lead to renal transplantation. Biological analysis may show rheumatoid factor or anti-neutrophil cytoplasmic antibodies [56, 63].

Pulmonary manifestations are almost constant in symptomatic carriers and include recurrent DAH. ILD without DAH may progress to end-stage lung fibrosis [65]. Diagnostic wandering and diagnosis of recurrent infectious pneumonia is common in children [65].

CT scan findings are similar to those reported in SAVI syndrome, namely features suggestive of DAH (ground-glass opacities) in addition to septal thickening, reticular opacities or cysts, and signs of fibrosis (traction bronchiectasis, honeycombing and volume loss) (figure 5) [57, 66]. BAL may confirm the diagnosis of DAH. A few histopathologic reports have reported DAH or unclassifiable fibrosing ILD (alveolar wall thickening, alveolar distortion, alveolitis and fibrosis) associated with lymphoid follicles with germinal-centre organisation, infiltrating T-cells and capillaritis with neutrophils within the alveolar septa [67, 68].

Although poorly reported, conventional immunosuppressants such as prednisone have shown some efficacy. In addition, JAK1/2 (ruxolitinib) and JAK1/3 (tofacitinib) inhibitors show promise. Lung transplant is limited to a very small number of cases and only feasible in the absence of contraindications such as extrapulmonary organ failure [56, 57, 63, 68–70].

PAP

PAP is a rare condition characterised by alveolar accumulation of surfactant [71]. Autoimmune PAP is more frequent, affecting more than 90% of PAP patients, and characterised by the presence of pathogenic anti-granulocyte–macrophage colony-stimulating factor (GM-CSF) autoantibodies. In addition to autoimmune PAP and PAP secondary to toxic inhalation, there are several causes of monogenic PAP. They are usually diagnosed in children and include the SRG pathogenic variant discussed above. However, the PAP pattern is usually a minor sign, often superimposed with more complex histopathology [17].

The classical hereditary form of PAP is related to homozygous mutations of *CSF2RA* and *CSF2RB*, which encode the α and β chains of the GM-CSF receptor. Two other genetic forms have emerged during the last decade, namely PAP associated with mutations in cytosolic tRNA synthetases, especially *MARS1*, and PAP related to *GATA2* mutations. Other inherited causes of PAP include *STAT5B* (encoding a protein that mediates signalling by GM-CSF or other cytokines), *ADA1*, *ADA2*, *IRF8*, *SLC7A7* (causing lysinuric protein intolerance), *OAS1* and *CCR2* (required for normal myeloid lineage development), which are thought to cause PAP by reducing the functions and/or numbers of alveolar macrophages, all being exceptional [72–79].

CS2FRA *and* CSF2RB

The most common PAP mutations are associated with genes encoding the α and β subunits of the GM-CSF receptor (*CSF2RA* and *CSF2RB*), although a small number of cases have been reported mostly in children with autosomal recessive transmission [80–82].

Most patients are diagnosed before the age of 10 without extrapulmonary manifestations but with failure to thrive. Routine blood tests and anti-GM-CSF antibodies are normal [83].

CT scans show a diffuse crazy-paving pattern with bilateral ground-glass opacities and sharply demarcated margins. Signs of pulmonary fibrosis may appear secondarily but are very unusual in GM-CSF receptor mutations, unlike in *MARS1* mutation carriers where it is almost constant at an early age, often before 10 years old (figure 6) [83]. The diagnosis of PAP is confirmed by BAL. When performed at diagnosis, lung biopsies show PAP similar to autoimmune PAP without interstitial abnormalities, but BAL is sufficient to diagnose PAP.

Whole-lung lavage therapy is usually effective, but patients may progress to pulmonary fibrosis and require lung or bone marrow transplantation or both [83, 84]. Intra-alveolar gene-pulmonary macrophage transplantation therapy has shown promising results in *CSF2RA*-knockout mice and is currently the subject of a prospective clinical trial in humans [84].

MARS1 *and other tRNA synthetases*

A genetic cause of PAP was suspected on La Réunion Island with the description of 32 family-connected cases of PAP. This was eventually linked to pathogenic *MARS1* variants of autosomal recessive transmission encoding the cytosolic methionyl-tRNA synthetase [85, 86].

PAP related to *MARS1* variants is frequently associated with extrapulmonary disease, with complete penetrance. At least seven different variants and around 50 patients have been reported [87].

The median age at diagnosis is 9 months (4 months−39 years). Failure to thrive and liver involvement (elevated liver enzymes and steatosis hepatomegaly) are frequent (56–89%).

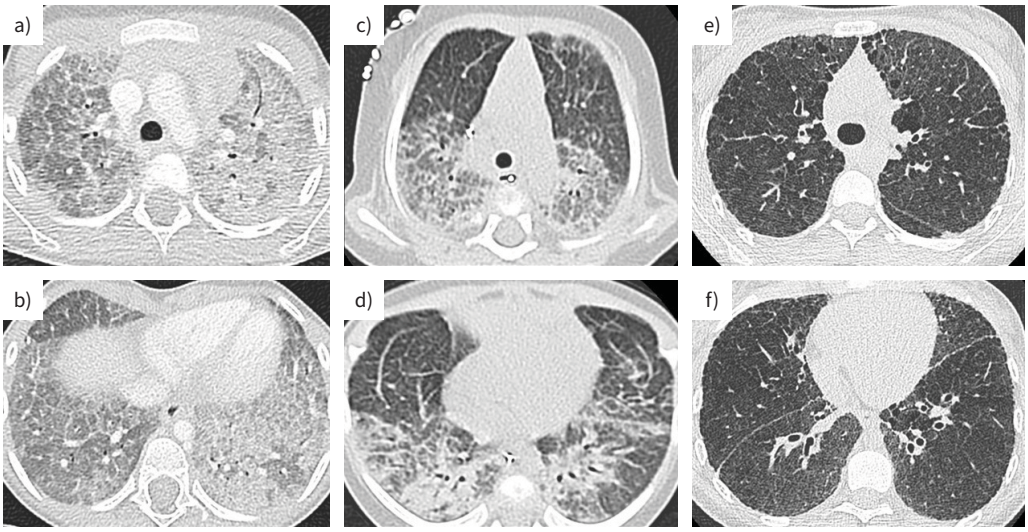

FIGURE 6 Computed tomography (CT) patterns associated with *CSF2RA* deficiency and *MARS* mutation. a and b) 6-year-old girl with *CSF2RA* deficiency. The CT scan reveals a diffuse crazy-paving pattern characterised by thickened interlobular septa and intralobular lines, superimposed with asymmetric ground-glass opacities, without zone predilection or gradient. Subsequently, almost complete regression of pulmonary alveolar proteinosis occurred after a phenoidentical bone marrow transplant. c and d) CT scan performed at the age of 2.5 months of a male with *MARS* mutation showing an anteroposterior density gradient with a crazy-paving pattern predominant in the posterior territories and distension in the anterior territories. e and f) The disease progressed to fibrosing interstitial pneumonia with CT at 12 years showing traction bronchiectasis and subpleural cysts with a honeycombing aspect.

The chest CT scan typically shows a symmetrical crazy-paving pattern (94%), in addition to posterobasal consolidations in 76% of cases (figure 6) [88]. BAL has a milky appearance and cytologic analysis shows large foamy periodic acid Schiff stain-positive macrophages and extracellular granular eosinophilic material (figure 6). Histopathology shows PAP lesions superimposed with lymphocyte infiltrates (84%), alveolar cholesterol granulomas and signs suggestive of fibrosis (50%).

Mortality was 59% in the series reports by Enaud *et al.* [86] and one quarter died before the age of 2 years. Patients usually present with progressive fibrosis and may require pulmonary transplantation [89].

Patients may experience partial improvement with whole lung lavage [90]. The addition of methionine increases *MARS* activity *in vitro* and oral supplementation has shown complete remission of the disease when initiated at diagnosis in a prospective clinical trial [90].

Homozygous mutations in genes encoding other cytosolic tRNA synthetases are responsible for multisystemic phenotypes that include an ILD [91]; mutations in *YARS1*, *LARS1*, *AARS1*, *IARS1* and *FARS1* are associated with various degrees of ILD from PAP to DAH to severe fibrosis [91–93].

GATA2

Several other genetic causes of macrophage dysfunction causing immune deficiency may also present with a PAP pattern [80, 81]. However, *GATA2* deficiency seems to be more frequently associated with PAP compared to other genetic causes of macrophage dysfunction.

Around 150 different variants (with three recurrent missense variants) have been reported with autosomal dominant transmission and frequent *de novo* mutations. The variants lead to decreased multilineage progenitors of B- and natural killer (NK) cells and to cytopenias and opportunistic infections. Penetrance and onset of disease are highly variable, even among individuals in the same kindred with identical *GATA2* variants [94].

The disease was initially named MonoMAC syndrome due to it being characterised by a reduced monocyte count and infection with *Mycobacterium avium* complex. Disease onset is usually in late adolescence or early adulthood, with nontuberculous mycobacterial, fungal or papillomavirus infections. Blood analysis reveals low B-cells, NK cells and monocytes. Haematological involvement may progress to myelodysplastic syndrome, chronic myelomonocytic leukaemia and acute myeloid leukaemia [95].

In a retrospective cohort of 124 patients, 56% showed reported lung involvement. CT scans showed small nodules (54%), reticular opacities (40%), emphysema (25%), ground-glass opacities (35%) and consolidations (21%). The crazy-paving pattern was rare (7%) (figure 7). The BAL analysis reported lymphocytic alveolitis (21%±23%) in addition to PAP [73]. Lung biopsies showed chronic lymphohistiocytic infiltration with scattered eosinophils in addition to PAP, but no granuloma formation [73].

Patients died within 2–20 years from disseminated infection or haematological progression [95]. Both haematological and pneumological involvement are improved with allogeneic hematopoietic stem cell transplantation [73, 95].

Cystic lung disease

Tuberous sclerosis complex (TSC)

TSC is the second most frequent phakomatosis after neurofibromatosis type I with a prevalence of 1:25 000 [96]. TSC is an autosomal dominant disorder caused by heterozygous mutations in *TSC1* or *TSC2* [97], two tumour-suppressor genes that cause activation of the mammalian target of rapamycin (mTOR) pathway. Of note, two-thirds of cases are caused by *de novo* mutations [98].

TSC can potentially affect all organs [99]. TSC is characterised by hamartomas in different organs, including the brain, lungs, skin, kidneys, heart and eyes. Manifestations usually follow an age-related expression, with skin lesions at birth and renal angiomyolipomas and lymphangioleiomyomatosis (LAM) appearing in adulthood [100]. Dermatological and oral lesions include hypomelanotic macules (or hypopigmented macules, also known as ash-leaf spots) (~90% of TSC patients), angiofibromas (especially in the central areas of the face) (~75%), ungual fibromas (~80%) and shagreen patches (~50%). Dental enamel pits are encountered in virtually all TSC patients and oral fibromas in approximately half of them [101]. The more frequent renal manifestation of TSC is angiomyolipomas, although they can also be found in the liver, uterus and, exceptionally, in the lungs [102]. Angiomyolipomas are present in 9% of TSC patients before the age of 2 and in 79% after the age of 40 [103]. TSC patients have an increased risk

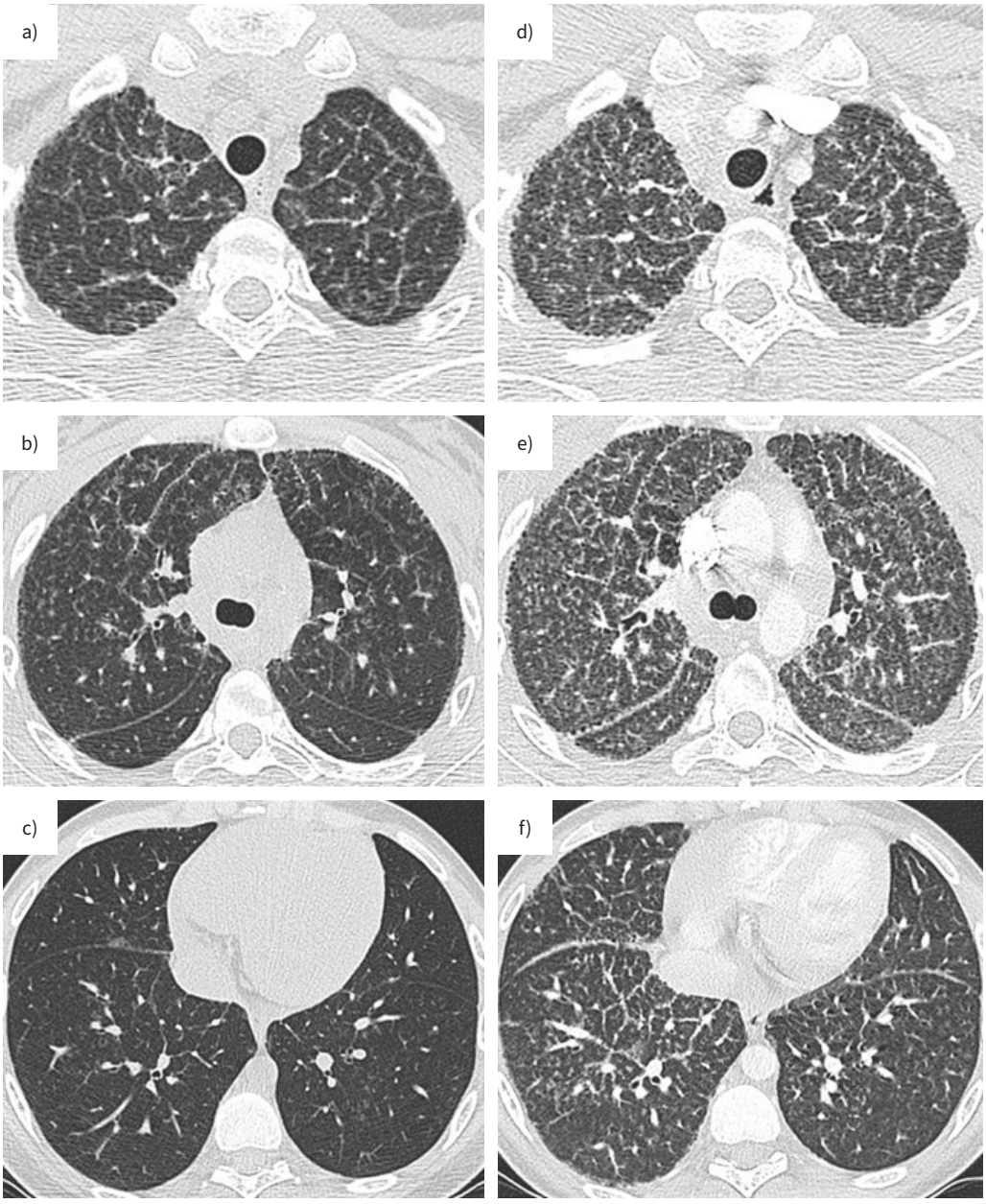

FIGURE 7 Computed tomography (CT) patterns associated with *GATA2* deficiency. a, b and c) 15-year-old girl with a past history of cytomegalovirus pneumonia in infancy, diagnosed with pancytopenia and myelodysplasia one year before presenting with progressive exertional dyspnoea. The CT scan reveals coarse thickening of the interlobular septa, intralobular lines, initially predominant in the upper lobes. Cystic lesions are observed along the pleura and interlobular septa. Bronchoalveolar lavage suggested alveolar proteinosis. d, e and f) A follow-up CT scan at 18 months showed a worsening of all previously described lesions and the overall extent of the disease, particularly the cystic lesions, that led to the patient's death 2 months later after bone marrow transplantation.

of renal cell carcinoma [104]. The neurological and neuropsychiatric features of TSC generate the greatest burden of the disease. The majority of affected individuals have structural brain lesions that include cortical tubers, subependymal nodules, subependymal giant cell astrocytoma, radial migration lines and retinal astrocytic hamartomas. Epilepsy is present in 70–90% of affected individuals and usually appears within the first year of life. TSC-associated neuropsychiatric disorders include intellectual disability, developmental delay, autism spectrum disorders and mood disorders [105].

Almost half of female TSC patients have cystic lung changes suggestive of LAM on systematic CT scans, but only 10% have symptomatic LAM (figure 8) [106]. LAM affects 10–38% of male TSC patients [107]. Characteristic CT scans show multiple, bilateral, round, well-defined, relatively uniform, thin-walled cysts with a diffuse distribution [108].

Other thoracic features include multifocal micronodular pneumocyte hyperplasia, pneumothoraces and lymphatic manifestations. Multifocal micronodular pneumocyte hyperplasia refers to the nodular proliferation of type II pneumocytes along the alveolar septa. On a CT scan it appears as multiple solid, semi-solid or ground glass nodules, sometimes with a target appearance. They range in size from 1 to 10 mm and are usually upper-lobe predominant and peripheral [109]. Multifocal micronodular pneumocyte hyperplasia is usually indolent and nonprogressive but it needs to be differentiated from premalignant pulmonary lesions [109]. Pneumothorax affects 55–73% of LAM patients with a relapse rate of 70% without surgery [110]. Lymphatic manifestations include chylothorax, chylous lung congestion, mediastinal adenomegalies and mediastinal and/or retroperitoneal lymphangioleiomyomas [110].

TSC patients have a reduced estimated life expectancy of 70 years and 63 years for TSC LAM [99]. mTOR inhibitors, such as sirolimus, stabilise lung function in LAM patients, in addition to benefits in terms of chylous effusion and lymphangiomas [111, 112].

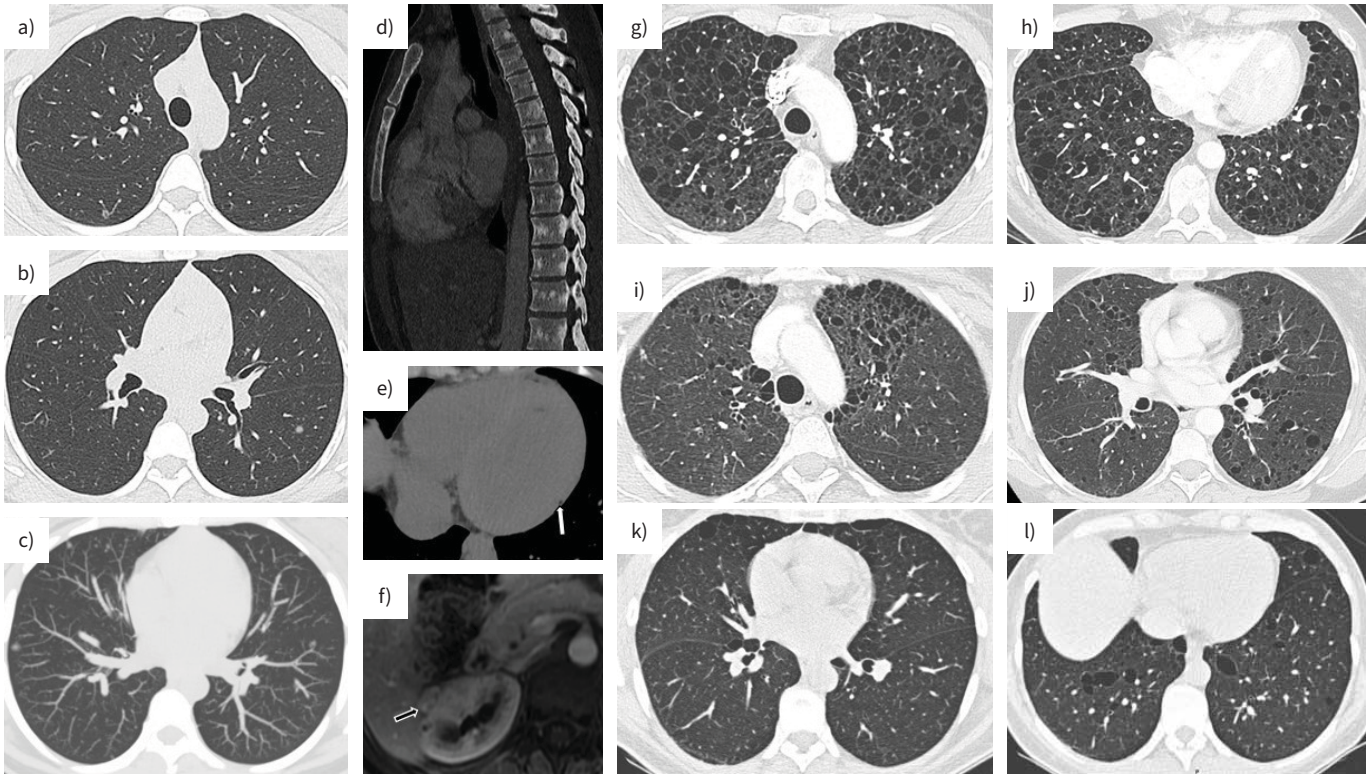

FIGURE 8 Computed tomography (CT) patterns of cystic lung disease of genetic origin. a, b and c) 31-year-old woman with confirmed tuberous sclerosis complex. CT shows multiple bilateral solid and nonsolid small lung nodules (displayed with maximum intensity projection, c) suggesting multifocal micronodular pneumocyte hyperplasia, associated with a few small lung cysts and multiple sclerotic lesions of the thoracic and lumbar vertebrae (sagittal view, d). A few fatty foci are visible in the myocardium on the unenhanced chest CT (white arrow, e) and the magnetic resonance imaging shows an enhancing right renal nodule related to a lipid-poor angiomyolipoma (black arrow, f). g and h) 48-year-old woman with tuberous sclerosis complex–lymphangioleiomyomatosis with characteristic bilateral, round, well-defined, uniform, thin-walled cysts with diffuse distribution. i and j) 46-year-old smoking woman with known neurofibromatosis type 1 disease and numerous upper lobe-predominant lung cysts that remained stable over 7 years of follow-up; however, she developed pulmonary hypertension that led to lung transplantation and death. k and l) 49-year-old woman with asymptomatic cystic lung disease revealing Birt–Hogg–Dubé syndrome. The cysts are characteristically lenticular in shape, located along the pleura and bronchovascular bundles, with a predominantly basal distribution.

Neurofibromatosis type 1 (NF1)

NF1, also known as von Recklinghausen disease, is an autosomal dominant disorder caused by mutations in the tumour suppressor *neurofibromin 1 (NF1)*, with a prevalence of 1:3000 to 1:6000 [113–116]. Approximately half of all cases result from *de novo* mutations [114]. NF1 diagnosis requires meeting two or more out of the seven National Institute of Health Consensus Development Conference criteria, namely 1) six or more café au lait macules, 2) two or more cutaneous or subcutaneous neurofibromas or one plexiform neurofibroma, 3) axillary or groin freckling, 4) optic pathway glioma, 5) two or more Lisch nodules, 6) bony dysplasia and 7) an NF1 first-degree relative [117].

The features of the disease are extremely variable and respiratory complications can develop progressively over a lifetime. These include pulmonary hypertension, ILD, airway plexiform neurofibromas and intrathoracic meningoceles [118]. Pulmonary hypertension is a rare but severe complication of NF1 [119]. Although ILD has not been the subject of a recent specific work, there seems to be a specific association with lung cysts. In a recent series of 41 NF1 patients, diffuse lung cysts were reported in 76% of cases on CT scans, in addition to ground-glass opacities (73%), emphysema (49%) and reticulations (39%) without topography preference (figure 8). These findings were also associated with possible radiologic signs of pulmonary hypertension. Differentiating cysts from emphysema may be difficult. The association of lung cysts, ground-glass opacities and emphysema was reported in one-third of cases. No fibrotic pattern was reported. ILD does not seem to lead to respiratory failure.

Birt–Hogg–Dubé syndrome (BHD)

BHD is a rare inherited autosomal dominant disorder with a prevalence of 1–9:1 000 000 and caused by mutations in the tumour suppressor gene *FLCN* coding for folliculin [120, 121]. Manifestations include cutaneous fibrofolliculomas, renal tumours of various histological types and multiple pulmonary cysts, with wide phenotypic variability. Patients can present with any combination of skin, pulmonary or renal manifestations of varying degrees of severity, even within the same family.

More than 80% of BHD patients present with multiple bilateral pulmonary cysts (figures 2 and 8) [122–124]. The cysts can vary in size, shape and number, but are typically thin-walled and predominantly distributed in the basal and subpleural or paramediastinal regions of the lung with a normal-appearing surrounding parenchyma [125, 126]. Cysts may have a lenticular shape and a central peribronchovascular distribution. The presence of cysts predisposes to spontaneous pneumothorax, with an incidence 50-fold higher than in the general population and a high recurrence rate [124]. Pleurodesis is therefore recommended after the first episode of pneumothorax [127]. Pulmonary cysts are usually asymptomatic or only associated with mild exertional dyspnoea [128]. Cystic lung disease in BHD has not been reported as leading to respiratory failure [128].

Miscellaneous

Pulmonary alveolar microlithiasis

Pulmonary alveolar microlithiasis is autosomal recessive disorder caused by *SLC34A2* mutations with around 1000 patients reported [98]. *SLC34A2* encodes the sodium-dependent phosphate transport protein 2B [129]. The disease is characterised by deposition of calcium phosphate concretions (microliths) in the alveoli. The mean age at diagnosis is usually between 20 and 40 years without gender predominance. Blood levels of calcium and phosphate are usually within normal levels. Kidney and gallbladder stones, as well as male genital apparatus calcifications, have been reported.

At the early stage of the disease, the radiological pattern is not typical due to the small number and lesser calcification of the microliths, showing ground-glass opacities, fine low-attenuating micronodules and reticular opacities.

The typical CT pattern shows numerous calcified micronodules diffusely distributed in both lungs and resulting in a “sand-like appearance”, predominating in the lower and posterior lung zones (figure 9). The micronodules are typically<1 mm, clearly outlined and bright. They may predominantly accumulate along the pleura and interlobular septa, corresponding to a perilobular distribution of microliths, or they may spare the subpleural region, appearing alongside small cysts or paraseptal emphysema. They evolve towards confluence over time and may show large calcified nodules or areas of calcified parenchyma. BAL and biopsy may show characteristic calciospherocitis (microliths) in the alveoli, but chest CT is usually sufficient to make the diagnosis and BAL is performed to exclude any other disease.

The clinical course is variable. In some patients, the disease remains quiescent while in others it progresses to respiratory insufficiency and early death. There may be a clinico–radiological dissociation with

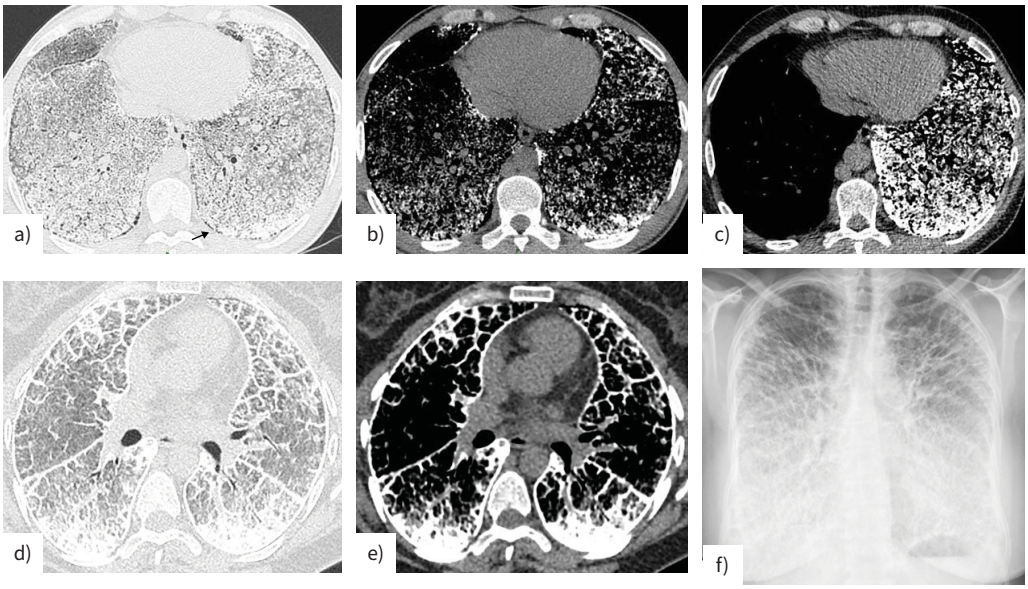

FIGURE 9 Computed tomography (CT) patterns associated with alveolar microlithiasis. a, b and c) 36-year-old male patient referred for lung transplantation for alveolar microlithiasis. a, b) The chest CT scan shows diffuse ground-glass opacities superimposed with scattered calcified micronodules, predominantly affecting the lower and posterior zones. A few subpleural cysts are visible in the lower lobes (arrow). c) 9 years later, following a right lung transplantation, the number of calcified nodules has increased in the native lung. d, e and f) 41-year-old female patient with a familial history of alveolar microlithiasis. d and e) The chest CT scan shows extensive calcifications along the pleura and alveolar septa, with large calcified areas in the posterior and inferior zones of both lungs. f) The septal and basal predominance of the calcifications is well depicted on the chest radiograph.

widespread pulmonary opacities on CT and mild functional impairment. Lung transplantation is currently the only effective therapy [130].

Other exceptional genetic interstitial lung diseases

A few other syndromes have been reported, including pulmonary fibrosis associated with other genes and pathways (figure 9) [2]. They are even more exceptional, seem to be limited to a very few families worldwide and include the following:

- Fibrosis, neurodegeneration and cerebral angiomatosis secondary to *NHLRC2* mutations.
- Poikilodermia and lung fibrosis secondary to *FAM111B* mutations (figure 10a–c).
- Prolidase deficiency secondary to *PEPD* mutations.
- Fanconi renotubular syndrome 5 (mitochondrial respiratory chain complex deficiency) secondary to *NDUFAF6* mutations.
- Trisomy 21, particularly when the patient is born prematurely, may manifest with small subpleural cysts. Rarely pulmonary fibrosis may develop (figure 9d–e).
- Werner syndrome secondary to *WRN* mutations.
- Patients with filamin A deficiency due to *FLNA* variants may develop lobular emphysematous or large cystic lesions in addition to periventricular nodular heterotopia often associated with seizures and cardiovascular structural abnormalities (figure 9f–g).
- *S100A13/S100A3* mutations involved in the calcium pathway.
- *ZNFX1* variants lead to type I IFN related dysfunction with recurrent viral and mycobacterial infections, peripheral monocytosis, thrombocytopenia, hepatosplenomegaly, renal disease and interstitial pneumonitis (figure 10h–i) [131].

This list is not exhaustive and is expected to grow in the future.

New candidate genes

Several whole-exome or genome analyses have been recently reported from IPF and FPF cohorts including more than 1000 patients [9, 10, 36, 132]. The prevalence of FPF genetically explained by known genes to cause ILD was disappointingly low as a rare variant was identified in only 25% of a cohort of 388 FPF patients [36]. However, several new candidate genes have been identified, highlighting new pathways involved in ILD.

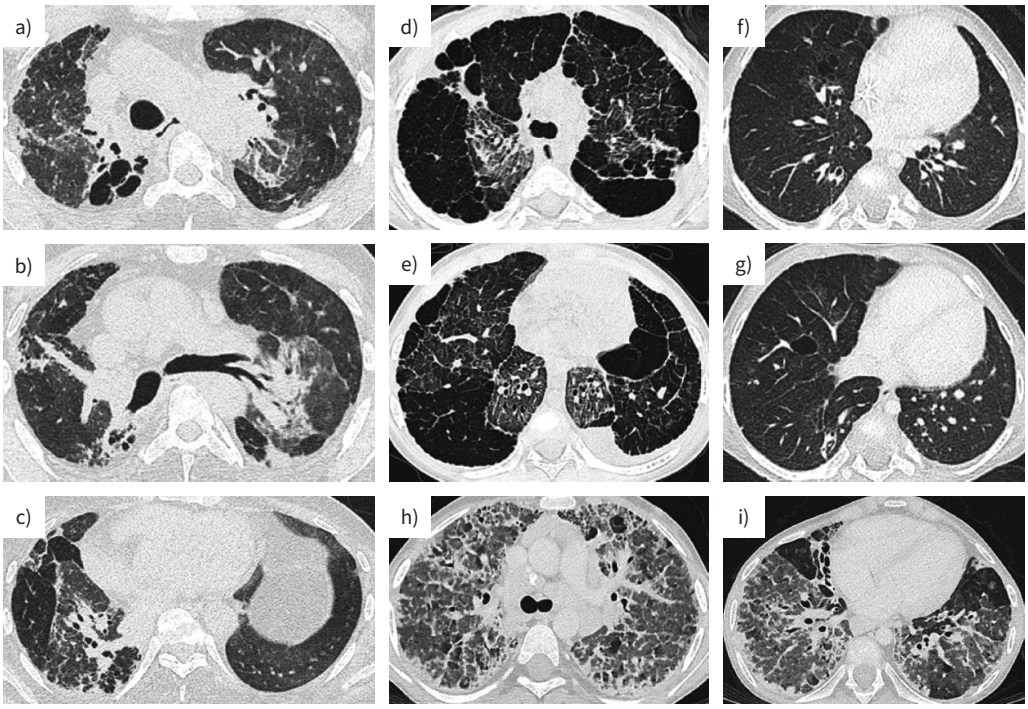

FIGURE 10 Computed tomography (CT) pattern of lung disease caused by genetic variants in *FAM111B*, trisomy 21 or variants in filamin A and *ZNFX1*. a–c) 30-year-old man referred for lung transplantation due to pulmonary fibrosis associated with hereditary fibrosing poikiloderma with tendon contractures and myopathy caused by an *FAM111B* mutation. The chest CT scan shows reticular and patchy ground-glass opacities, cystic lesions, small subpleural consolidations and associated massive distortion of the lung architecture, with important lower lobe volume loss. d and e) 5-year-old boy with trisomy 21 and pulmonary fibrosis. Lung developmental alveolar disorder characterised by large cystic lesions and hyperlucent zones in the subpleural regions. Diffuse septal thickening and mild ground-glass opacities are present in other zones. f and g) 2-year-old boy with chronic partial respiratory insufficiency due to *filamin A* mutation. The chest CT scan shows a few cysts in the right lung associated with discrete signs of lung distortion. The left lung has a reduced volume with an ipsilateral mediastinum shift. h and i) 10-year-old girl referred for lung transplant due to *ZNFX1* deficiency. The chest CT scan shows a diffuse fibrosing interstitial lung disease with predominant ground-glass opacities, associated reticular opacities, small cysts and traction bronchiectasis. Some hyperlucent lobular or segmental zones are also present in both lungs, along with diffuse reticular opacities superimposed on ground-glass opacities, associated with small cysts and hyperlucent zones. Mild distortion of the fissures and traction bronchiectasis in the middle lobe. There is a chest wall deformity (pectus carinatum).

Zhang *et al.* [36, 133] identified rare variants in *KIF15*, a kinesin involved in spindle separation during mitosis in 9% of the rare variants identified. In parallel, Liu *et al.* [10] identified *SYDE1* (n=2), *SERPINB8* (n=1), *GPR87* (n=2) and *NETO1* (n=2) as new candidate genes in 569 analysed families. Interestingly *SYDE1* is involved in cell migration and *SERPINB8* encodes for a serine protease also involved in cell–cell adhesion, suggesting that genes involved in cell interactions may play a role in the genetic landscape of FPF. Replication and functional studies are needed to confirm these results as well as a more precise report of the phenotypes.

Conclusion

Genetic analysis in ILD is a revolution in progress in the diagnosis and understanding of the physiopathology of diseases. However, these results are limited to a very small number of patients and families compared to the number of ILD and FPF patients. In addition, these results are unlikely to significantly modify the current management of patients. Given the low number of patients and the variety of diseases, it is unfortunately expected that there will be long delays before truly targeted treatments can be considered. Before considering therapeutic studies, the first step is to make radiological and genetic diagnoses of these patients.

The genetics of ILD is a rapidly evolving field, yet significant obstacles remain in achieving a deeper understanding. One major challenge is the heterogeneity of ILD, which encompasses a wide spectrum of disorders with varied genetic underpinnings. This complexity is compounded by the rarity of certain

genetic variants, making it difficult to gather large enough cohorts for meaningful studies. Additionally, limited access to genetic testing and differences in diagnostic criteria across regions further hinder progress. However, the future holds promise with the establishment of comprehensive registries, particularly across Europe. Such registries would, in collaboration with patients and relatives, consolidate data from multiple centres of excellence, enhancing the ability to identify and study rare genetic variants. This collaborative approach could significantly advance the drug development process, provide a robust platform for clinical trials and ultimately improve patient outcomes.

Point for clinical practice

- The radiological pattern of genetically inherited ILDs can provide clues suggestive of a specific genetic cause, in addition to extrapulmonary manifestations.

Provenance: Submitted article, peer reviewed.

Conflict of interest: R. Borie reports consultancy fees from Boerhinger Ingelheim, Ferrer and Sanofi, payment or honoraria for lectures, presentations, manuscript writing or educational events from Boehringer Ingelheim, and support for attending meetings from Boehringer Ingelheim. L. Berteloot and C. Kannengiesser have nothing to disclose. M. Griese reports grants from Deutsche Forschungsgemeinschaft, and participation on a data safety monitoring board or advisory board with Boehringer Ingelheim. A. Cazes reports payment or honoraria for lectures, presentations, manuscript writing or educational events from Boehringer Ingelheim. B. Crestani reports grants from Boehringer Ingelheim, consultancy fees from BMS, Boehringer Ingelheim, Chiesi, CSL Behring, GSK and Sanofi, payment or honoraria for lectures, presentations, manuscript writing or educational events from AstraZeneca, BMS, Boehringer Ingelheim, GSK, Novartis, Roche and Sanofi, support for attending meetings from AstraZeneca, BMS, Boehringer Ingelheim, Roche and Sanofi, participation on a data safety monitoring board or advisory board with BMS, Boehringer Ingelheim, Horizon and Sanofi, and a leadership role with Fondation du Souffle (President of the board of trustees). A. Hadchouel has nothing to disclose. M.P. Debray reports consultancy fees from Boehringer Ingelheim, payment or honoraria for lectures, presentations, manuscript writing or educational events from Boehringer Ingelheim, Sanofi and Bracco, and support for attending meetings from Boehringer Ingelheim.

References

1 Newton CA, Oldham JM, Applegate C, *et al.* The role of genetic testing in pulmonary fibrosis: a perspective from the Pulmonary Fibrosis Foundation Genetic Testing Work Group. *Chest* 2022; 162: 394–405.
2 Borie R, Kannengiesser C, Antoniou K, *et al.* European Respiratory Society statement on familial pulmonary fibrosis. *Eur Respir J* 2023; 61: 2201383.
3 Borie R, Tabeze L, Thabut G, *et al.* Prevalence and characteristics of *TERT* and *TERC* mutations in suspected genetic pulmonary fibrosis. *Eur Respir J* 2016; 48: 1721–1731.
4 Juge P-A, Lee JS, Ebstein E, *et al. MUC5B* promoter variant and rheumatoid arthritis with interstitial lung disease. *N Engl J Med* 2018; 379: 2209–2219.
5 Thouvenin G, Abou Taam R, Flamein F, *et al.* Characteristics of disorders associated with genetic mutations of surfactant protein C. *Arch Child* 2010; 95: 449–454.
6 Whitsett JA, Wert SE, Weaver TE. Alveolar surfactant homeostasis and the pathogenesis of pulmonary disease. *Annu Rev Med* 2010; 61: 105–119.
7 Li Y, Seidl E, Knoflach K, *et al. ABCA3*-related interstitial lung disease beyond infancy. *Thorax* 2023; 78: 587–595.
8 Lawson WE, Grant SW, Ambrosini V, *et al.* Genetic mutations in surfactant protein C are a rare cause of sporadic cases of IPF. *Thorax* 2004; 59: 977–980.
9 Sutton RM, Bittar HT, Sullivan DI, *et al.* Rare surfactant-related variants in familial and sporadic pulmonary fibrosis. *Hum Mutat* 2022; 43: 2091–2101.
10 Liu Q, Zhou Y, Cogan JD, *et al.* The genetic landscape of familial pulmonary fibrosis. *Am J Respir Crit Care Med* 2023; 207: 1345–1357.
11 Nattes E, Lejeune S, Carsin A, *et al.* Heterogeneity of lung disease associated with NK2 homeobox 1 mutations. *Respir Med* 2017; 129: 16–23.
12 Diesler R, Legendre M, Si-Mohamed S, *et al.* Similarities and differences of interstitial lung disease associated with pathogenic variants in *SFTPC* and *ABCA3* in adults. *Respirology* 2024; 29: 312–323.
13 Brudon A, Legendre M, Mageau A, *et al.* High risk of lung cancer in surfactant-related gene variant carriers. *Eur Respir J* 2024; 63: 2301809.
14 Campo I, Zorzetto M, Mariani F, *et al.* A large kindred of pulmonary fibrosis associated with a novel ABCA3 gene variant. *Respir Res* 2014; 15: 43.
15 van Moorsel CH, van Oosterhout MF, Barlo NP, *et al.* Surfactant protein C mutations are the basis of a significant portion of adult familial pulmonary fibrosis in a Dutch cohort. *Am J Respir Crit Care Med* 2010; 182: 1419–1425.

16 Klay D, Platenburg M, van Rijswijk R, *et al.* ABCA3 mutations in adult pulmonary fibrosis patients: a case series and review of literature. *Curr Opin Pulm Med* 2020; 26: 293–301.
17 Legendre M, Butt A, Borie R, *et al.* Functional assessment and phenotypic heterogeneity of *SFTPA1* and *SFTPA2* mutations in interstitial lung diseases and lung cancer. *Eur Respir J* 2020; 56: 2002806.
18 Borie R, Funalot B, Epaud R, *et al. NKX2*.1 (TTF1) germline mutation associated with pulmonary fibrosis and lung cancer. *ERJ Open Res* 2021; 7: 00356-02021.
19 Abou Taam R, Jaubert F, Emond S, *et al.* Familial interstitial disease with I73 T mutation: a mid- and long-term study. *Pediatr Pulmonol* 2009; 44: 167–175.
20 Kroner C, Reu S, Teusch V, *et al.* Genotype alone does not predict the clinical course of *SFTPC* deficiency in paediatric patients. *Eur Respir J* 2015; 46: 197–206.
21 Flamein F, Riffault L, Muselet-Charlier C, *et al.* Molecular and cellular characteristics of *ABCA3* mutations associated with diffuse parenchymal lung diseases in children. *Hum Mol Genet* 2012; 21: 765–775.
22 Klay D, Hoffman TW, Harmsze AM, *et al.* Systematic review of drug effects in humans and models with surfactant-processing disease. *Eur Respir Rev* 2018; 27: 170135.
23 Klay D, Grutters JC, van der Vis JJ, *et al.* Progressive disease with low survival in adult patients with pulmonary fibrosis carrying surfactant-related gene mutations: an observational study. *Chest* 2023; 163: 870–880.
24 Bermudez J, Nathan N, Coiffard B, *et al.* Outcome of lung transplantation for adults with interstitial lung disease associated with genetic disorders of the surfactant system. *ERJ Open Res* 2023; 9: 00240-2023.
25 Calado RT, Young NS. Telomere diseases. *N Engl J Med* 2009; 361: 2353–2365.
26 Stanley SE, Gable DL, Wagner CL, *et al.* Loss-of-function mutations in the RNA biogenesis factor *NAF1* predispose to pulmonary fibrosis–emphysema. *Sci Transl Med* 2016; 8: 351ra107.
27 Newton CA, Batra K, Torrealba J, *et al.* Telomere-related lung fibrosis is diagnostically heterogeneous but uniformly progressive. *Eur Respir J* 2016; 48: 1710–1720.
28 Fernandez BA, Fox G, Bhatia R, *et al.* A Newfoundland cohort of familial and sporadic idiopathic pulmonary fibrosis patients: clinical and genetic features. *Respir Res* 2012; 13: 64.
29 Diaz de Leon A, Cronkhite JT, Katzenstein AL, *et al.* Telomere lengths, pulmonary fibrosis and telomerase (*TERT*) mutations. *PLoS One* 2010; 5: e10680.
30 Alder JK, Parry EM, Yegnasubramanian S, *et al.* Telomere phenotypes in females with heterozygous mutations in the dyskeratosis congenita 1 (*DKC1*) gene. *Hum Mutat* 2013; 34: 1481–1485.
31 Fukuhara A, Tanino Y, Ishii T, *et al.* Pulmonary fibrosis in dyskeratosis congenita with *TINF2* gene mutation. *Eur Respir J* 2013; 42: 1757–1759.
32 Alder JK, Stanley SE, Wagner CL, *et al.* Exome sequencing identifies mutant *TINF2* in a family with pulmonary fibrosis. *Chest* 2015; 147: 1361–1368.
33 Stuart BD, Choi J, Zaidi S, *et al.* Exome sequencing links mutations in *PARN* and *RTEL1* with familial pulmonary fibrosis and telomere shortening. *Nat Genet* 2015; 47: 512–517.
34 Cogan JD, Kropski JA, Zhao M, *et al.* Rare variants in *RTEL1* are associated with familial interstitial pneumonia. *Am J Respir Crit Care Med* 2015; 191: 646–655.
35 Kannengiesser C, Borie R, Menard C, *et al.* Heterozygous *RTEL1* mutations are associated with familial pulmonary fibrosis. *Eur Respir J* 2015; 46: 474–485.
36 Zhang D, Newton CA, Wang B, *et al.* Utility of whole genome sequencing in assessing risk and clinically relevant outcomes for pulmonary fibrosis. *Eur Respir J* 2022; 60: 2200577.
37 Niewisch MR, Beier F, Savage SA. Clinical manifestations of telomere biology disorders in adults. *Hematol Am Soc Hematol Educ Program* 2023; 2023: 563–572.
38 Philippot Q, Kannengiesser C, Debray MP, *et al.* Interstitial lung diseases associated with mutations of poly (A)-specific ribonuclease: a multicentre retrospective study. *Respirology* 2022; 27: 226–235.
39 Sidali S, Borie R, de Fontbrune FS, *et al.* Liver disease in germline mutations of telomere-related genes: prevalence, clinical, radiological, pathological features, outcome, and risk factors. *Hepatology* 2023; 79: 1365–1380.
40 Karimi-Shah BA, Chowdhury BA. Forced vital capacity in idiopathic pulmonary fibrosis–FDA review of pirfenidone and nintedanib. *N Engl J Med* 2015; 372: 1189–1191.
41 Dressen A, Abbas AR, Cabanski C, *et al.* Analysis of protein-altering variants in telomerase genes and their association with *MUC5B* common variant status in patients with idiopathic pulmonary fibrosis: a candidate gene sequencing study. *Lancet Respir Med* 2018; 6: 603–614.
42 McGovern MM, Wasserstein MP, Aron A, *et al.* Ocular manifestations of Niemann–Pick disease type B. *Ophthalmology* 2004; 111: 1424–1427.
43 Alexander WS. Niemann–Pick disease; report of a case showing calcification in the adrenal glands. *N Z Med J* 1946; 45: 43–45.
44 Mendelson DS, Wasserstein MP, Desnick RJ, *et al.* Type B Niemann–Pick disease: findings at chest radiography, thin-section CT, and pulmonary function testing. *Radiology* 2006; 238: 339–345.
45 Freitas HMP, Mançano AD, Rodrigues RS, *et al.* Niemann–Pick disease type B: HRCT assessment of pulmonary involvement. *J Bras Pneumol* 2017; 43: 451–455.

46 Guillemot N, Troadec C, de Villemeur TB, *et al.* Lung disease in Niemann–Pick disease. *Pediatr Pulmonol* 2007; 42: 1207–1214.
47 Wasserstein M, Lachmann R, Hollak C, *et al.* A randomized, placebo-controlled clinical trial evaluating olipudase alfa enzyme replacement therapy for chronic acid sphingomyelinase deficiency (ASMD) in adults: one-year results. *Genet Med* 2022; 24: 1425–1436.
48 Nalysnyk L, Rotella P, Simeone JC, *et al.* Gaucher disease epidemiology and natural history: a comprehensive review of the literature. *Hematology* 2017; 22: 65–73.
49 Goitein O. Lung involvement and enzyme replacement therapy in Gaucher's disease. *QJM* 2001; 94: 407–415.
50 Zarate YA, Hopkin RJ. Fabry's disease. *Lancet* 2008; 372: 1427–1435.
51 Wei ML. Hermansky–Pudlak syndrome: a disease of protein trafficking and organelle function. *Pigment Cell Res* 2006; 19: 19–42.
52 Nakatani Y, Nakamura N, Sano J, *et al.* Interstitial pneumonia in Hermansky–Pudlak syndrome: significance of florid foamy swelling/degeneration (giant lamellar body degeneration) of type-2 pneumocytes. *Virchows Arch Int J Pathol* 2000; 437: 304–313.
53 Hengst M, Naehrlich L, Mahavadi P, *et al.* Hermansky–Pudlak syndrome type 2 manifests with fibrosing lung disease early in childhood. *Orphanet J Rare Dis* 2018; 13: 42.
54 Benvenuto L, Qayum S, Kim H, *et al.* Lung transplantation for pulmonary fibrosis associated with Hermansky–Pudlak syndrome. A single-center experience. *Transplant Direct* 2022; 8: e1303.
55 Georgin-Lavialle S, Ducharme-Benard S, Sarrabay G, *et al.* Systemic autoinflammatory diseases: clinical state of the art. *Best Pract Res Clin Rheumatol* 2020; 34: 101529.
56 Liu Y, Jesus AA, Marrero B, *et al.* Activated STING in a vascular and pulmonary syndrome. *N Engl J Med* 2014; 371: 507–518.
57 Volpi S, Tsui J, Mariani M, *et al.* Type I interferon pathway activation in COPA syndrome. *Clin Immunol* 2018; 187: 33–36.
58 Rodríguez-Carrio J, Burska A, Conaghan PG, *et al.* Association between type I interferon pathway activation and clinical outcomes in rheumatic and musculoskeletal diseases: a systematic literature review informing EULAR points to consider. *RMD Open* 2023; 9: e002864.
59 David C, Frémond M-L. Lung inflammation in STING-associated vasculopathy with onset in infancy (SAVI). *Cells* 2022; 11: 318.
60 Berrada KR, Belot A, Neven B, *et al.* Lung transplantation under a Janus kinase inhibitor in three patients with SAVI syndrome. *J Clin Immunol* 2023; 43: 2156–2164.
61 Frémond M-L, Crow YJ. STING-mediated lung inflammation and beyond. *J Clin Immunol* 2021; 41: 501–514.
62 Frémond M-L, Hadchouel A, Berteloot L, *et al.* Overview of STING-associated vasculopathy with onset in infancy (SAVI) among 21 patients. *J Allergy Clin Immunol Pract* 2021; 9: 803–818.
63 Picard C, Thouvenin G, Kannengiesser C, *et al.* severe pulmonary fibrosis as the first manifestation of interferonopathy (*TMEM173* mutation). *Chest* 2016; 150: e65–e71.
64 Frémond M-L, Nathan N. COPA syndrome, 5 years after: where are we? *Joint Bone Spine* 2021; 88: 105070.
65 Frémond M-L, Legendre M, Fayon M, *et al.* Use of ruxolitinib in COPA syndrome manifesting as life-threatening alveolar haemorrhage. *Thorax* 2020; 75: 92–95.
66 Noorelahi R, Perez G, Otero HJ. Imaging findings of COPA syndrome in a 12-year-old boy. *Pediatr Radiol* 2018; 48: 279–282.
67 Tsui JL, Estrada OA, Deng Z, *et al.* Analysis of pulmonary features and treatment approaches in the COPA syndrome. *ERJ Open Res* 2018; 4: 00017-2018.
68 Vece TJ, Watkin LB, Nicholas S, *et al.* COPA syndrome: a novel autosomal dominant immune dysregulatory disease. *J Clin Immunol* 2016; 36: 377–387.
69 Frémond M-L, Rodero MP, Jeremiah N, *et al.* Efficacy of the Janus kinase 1/2 inhibitor ruxolitinib in the treatment of vasculopathy associated with *TMEM173*-activating mutations in 3 children. *J Allergy Clin Immunol* 2016; 138: 1752–1755.
70 Seo J, Kang J-A, Suh DI, *et al.* Tofacitinib relieves symptoms of stimulator of interferon genes (STING)-associated vasculopathy with onset in infancy caused by 2 *de novo* variants in *TMEM173*. *J Allergy Clin Immunol* 2017; 139: 1396–1399.
71 Trapnell BC, Nakata K, Bonella F, *et al.* Pulmonary alveolar proteinosis. *Nat Rev Dis Primer* 2019; 5: 16.
72 Xipell JM, Ham KN, Price CG, *et al.* Acute silicoproteinosis. *Thorax* 1977; 32: 104–111.
73 Marciano BE, Olivier KN, Folio LR, *et al.* Pulmonary manifestations of GATA2 deficiency. *Chest* 2021; 160: 1350–1359.
74 Rosain J, Bernasconi A, Prieto E, *et al.* Pulmonary alveolar proteinosis and multiple infectious diseases in a child with autosomal recessive complete IRF8 deficiency. *J Clin Immunol* 2022; 42: 975–985.
75 Zhang G, Cao L. New mutations in the *SLC7A7* gene of two Chinese sisters with lysinuric protein intolerance. *Pediatr Pulmonol* 2017; 52: E94–E96.
76 Grunebaum E, Cutz E, Roifman CM. Pulmonary alveolar proteinosis in patients with adenosine deaminase deficiency. *J Allergy Clin Immunol* 2012; 129: 1588–1593.

77 Tanaka T, Motoi N, Tsuchihashi Y, *et al.* Adult-onset hereditary pulmonary alveolar proteinosis caused by a single-base deletion in *CSF2RB*. *J Med Genet* 2011; 48: 205–209.
78 Krone K, Platt C, Pai S-Y, *et al.* STAT5b deficiency: a rare cause of pulmonary alveolar proteinosis. *Am J Respir Crit Care Med* 2019; 199: A2435.
79 Neehus A-L, Carey B, Landekic M, *et al.* Human inherited CCR2 deficiency underlies progressive polycystic lung disease. *Cell* 2024; 187: 390–408.
80 Hadchouel A, Drummond D, Abou Taam R, *et al.* Alveolar proteinosis of genetic origins. *Eur Respir Rev* 2020; 29: 190187.
81 Campo I. The influence of genetics on therapeutic developments in pulmonary alveolar proteinosis. *Curr Opin Pulm Med* 2019; 25: 294–299.
82 Papiris SA, Louvrier C, Fabre A, *et al. CSF2RB* mutation-related hereditary pulmonary alveolar proteinosis: the “long and winding road” into adulthood. *ERJ Open Res* 2023; 9: 00703-2023.
83 Suzuki T, Sakagami T, Young LR, *et al.* Hereditary pulmonary alveolar proteinosis: pathogenesis, presentation, diagnosis, and therapy. *Am J Respir Crit Care Med* 2010; 182: 1292–1304.
84 Arumugam P, Suzuki T, Shima K, *et al.* Long-term safety and efficacy of gene-pulmonary macrophage transplantation therapy of PAP in Csf2ra$^{-/-}$ mice. *Mol Ther* 2019; 27: 1597–1611.
85 Hadchouel A, Wieland T, Griese M, *et al.* Biallelic mutations of methionyl-tRNA synthetase cause a specific type of pulmonary alveolar proteinosis prevalent on Reunion Island. *Am J Hum Genet* 2015; 96: 826–831.
86 Enaud L, Hadchouel A, Coulomb A, *et al.* Pulmonary alveolar proteinosis in children on La Reunion Island: a new inherited disorder? *Orphanet J Rare Dis* 2014; 9: 85.
87 Castaldo A, Delestrain C, Diesler R, *et al.* Idiopathic pulmonary fibrosis with benign *SFTPC* variant and pathogenic *MARS1* mutations: can’t see the forest for the trees! *ERJ Open Res* 2023; 9: 00472-2023.
88 Berteloot L, Taam RA, Emond-Gonsard S, *et al.* Primary pulmonary alveolar proteinosis: computed tomography features at diagnosis. *Pediatr Radiol* 2014; 44: 795–802.
89 Roy C, Allou N, Coulomb A, *et al.* Successful lung transplantation in genetic methionyl-tRNA synthetase-related alveolar proteinosis/lung fibrosis without recurrence under methionine supplementation: medium-term outcome in 4 cases. *Am J Transplant* 2024; 24: 1317–1322.
90 Hadchouel A, Drummond D, Pontoizeau C, *et al.* Methionine supplementation for multi-organ dysfunction in MetRS-related pulmonary alveolar proteinosis. *Eur Respir J* 2022; 59: 2101554.
91 Fuchs SA, Schene IF, Kok G, *et al.* Aminoacyl-tRNA synthetase deficiencies in search of common themes. *Genet Med* 2019; 21: 319–330.
92 Charbit-Henrion F, Goguyer-Deschaumes R, Borensztajn K, *et al.* Systemic inflammatory syndrome in children with *FARSA* deficiency. *Clin Genet* 2022; 101: 552–558.
93 Schuch LA, Forstner M, Rapp CK, *et al.* FARS1-related disorders caused by bi-allelic mutations in cytosolic phenylalanyl-tRNA synthetase genes: look beyond the lungs! *Clin Genet* 2021; 99: 789–801.
94 Dickinson RE, Griffin H, Bigley V, *et al.* Exome sequencing identifies GATA-2 mutation as the cause of dendritic cell, monocyte, B and NK lymphoid deficiency. *Blood* 2011; 118: 2656–2658.
95 Calvo KR, Hickstein DD. The spectrum of GATA2 deficiency syndrome. *Blood* 2023; 141: 1524–1532.
96 Hallett L, Foster T, Liu Z, *et al.* Burden of disease and unmet needs in tuberous sclerosis complex with neurological manifestations: systematic review. *Curr Med Res Opin* 2011; 27: 1571–1583.
97 Curatolo P, Bombardieri R, Jozwiak S. Tuberous sclerosis. *Lancet* 2008; 372: 657–668.
98 Zöllner JP, Franz DN, Hertzberg C, *et al.* A systematic review on the burden of illness in individuals with tuberous sclerosis complex (TSC). *Orphanet J Rare Dis* 2020; 15: 23.
99 Northrup H, Aronow ME, Bebin EM, *et al.* Updated international tuberous sclerosis complex diagnostic criteria and surveillance and management recommendations. *Pediatr Neurol* 2021; 123: 50–66.
100 Auvin S, Bissler JJ, Cottin V, *et al.* A step-wise approach for establishing a multidisciplinary team for the management of tuberous sclerosis complex: a Delphi consensus report. *Orphanet J Rare Dis* 2019; 14: 91.
101 Rebaine Y, Nasser M, Girerd B, *et al.* Tuberous sclerosis complex for the pulmonologist. *Eur Respir Rev* 2021; 30: 200348.
102 Bissler JJ, Kingswood JC. Renal manifestation of tuberous sclerosis complex. *Am J Med Genet* 2018; 178: 338–347.
103 Kingswood JC, Belousova E, Benedik MP, *et al.* Renal angiomyolipoma in patients with tuberous sclerosis complex: findings from the TuberOus SClerosis registry to increase disease Awareness. *Nephrol Dial Transplant* 2019; 34: 502–508.
104 Trnka P, Kennedy SE. Renal tumors in tuberous sclerosis complex. *Pediatr Nephrol* 2021; 36: 1427–1438.
105 de Vries PJ, Wilde L, de Vries MC, *et al.* A clinical update on tuberous sclerosis complex-associated neuropsychiatric disorders (TAND). *Am J Med Genet C Semin Med Genet* 2018; 178: 309–320.
106 Cudzilo CJ, Szczesniak RD, Brody AS, *et al.* Lymphangioleiomyomatosis screening in women with tuberous sclerosis. *Chest* 2013; 144: 578–585.
107 Ryu JH, Sykes A-MG, Lee AS, *et al.* Cystic lung disease is not uncommon in men with tuberous sclerosis complex. *Respir Med* 2012; 106: 1586–1590.

108 Gupta N, Finlay GA, Kotloff RM, *et al.* Lymphangioleiomyomatosis diagnosis and management: high-resolution chest computed tomography, transbronchial lung biopsy, and pleural disease management. an Official American Thoracic Society/Japanese Respiratory Society clinical practice guideline. *Am J Respir Crit Care Med* 2017; 196: 1337–1348.

109 Konno S, Shigemura M, Ogi T, *et al.* Clinical course of histologically proven multifocal micronodular pneumocyte hyperplasia in tuberous sclerosis complex: a case series and comparison with lymphangiomyomatosis. *Respir Int Rev Thorac Dis* 2018; 95: 310–316.

110 Gupta N, Henske EP. Pulmonary manifestations in tuberous sclerosis complex. *Am J Med Genet C Semin Med Genet* 2018; 178: 326–337.

111 Hu S, Wu X, Xu W, *et al.* Long-term efficacy and safety of sirolimus therapy in patients with lymphangioleiomyomatosis. *Orphanet J Rare Dis* 2019; 14: 206.

112 McCormack FX, Inoue Y, Moss J, *et al.* Efficacy and safety of sirolimus in lymphangioleiomyomatosis. *N Engl J Med* 2011; 364: 1595–1606.

113 Huson SM, Compston DA, Clark P, *et al.* A genetic study of von Recklinghausen neurofibromatosis in South East Wales. I. Prevalence, fitness, mutation rate, and effect of parental transmission on severity. *J Med Genet* 1989; 26: 704–711.

114 Friedman JM. Epidemiology of neurofibromatosis type 1. *Am J Med Genet* 1999; 89: 1–6.

115 Lammert M, Friedman JM, Kluwe L, *et al.* Prevalence of neurofibromatosis 1 in German children at elementary school enrollment. *Arch Dermatol* 2005; 141: 71–74.

116 Uusitalo E, Leppävirta J, Koffert A, *et al.* Incidence and mortality of neurofibromatosis: a total population study in Finland. *J Invest Dermatol* 2015; 135: 904–906.

117 National Institutes of Health Consensus Development Conference Statement: neurofibromatosis. Bethesda, MD, USA, July 13–15, 1987. *Neurofibromatosis* 1988; 1: 172–178.

118 Jutant E-M, Girerd B, Jaïs X, *et al.* Pulmonary hypertension associated with neurofibromatosis type 1. *Eur Respir Rev* 2018; 27: 180053.

119 Jutant E-M, Jaïs X, Girerd B, *et al.* Phenotype and outcomes of pulmonary hypertension associated with neurofibromatosis type 1. *Am J Respir Crit Care Med* 2020; 202: 843–852.

120 Nickerson ML, Warren MB, Toro JR, *et al.* Mutations in a novel gene lead to kidney tumors, lung wall defects, and benign tumors of the hair follicle in patients with the Birt–Hogg–Dubé syndrome. *Cancer Cell* 2002; 2: 157–164.

121 Birt AR, Hogg GR, Dubé WJ. Hereditary multiple fibrofolliculomas with trichodiscomas and acrochordons. *Arch Dermatol* 1977; 113: 1674–1677.

122 Schmidt LS, Nickerson ML, Warren MB, *et al.* Germline BHD-mutation spectrum and phenotype analysis of a large cohort of families with Birt–Hogg–Dubé syndrome. *Am J Hum Genet* 2005; 76: 1023–1033.

123 Toro JR, Pautler SE, Stewart L, *et al.* Lung cysts, spontaneous pneumothorax, and genetic associations in 89 families with Birt–Hogg–Dubé syndrome. *Am J Respir Crit Care Med* 2007; 175: 1044–1053.

124 Zbar B, Alvord WG, Glenn G, *et al.* Risk of renal and colonic neoplasms and spontaneous pneumothorax in the Birt–Hogg–Dubé syndrome. *Cancer Epidemiol Biomarkers Prev* 2002; 11: 393–400.

125 Agarwal PP, Gross BH, Holloway BJ, *et al.* Thoracic CT findings in Birt–Hogg–Dube syndrome. *AJR Am J Roentgenol* 2011; 196: 349–352.

126 Tobino K, Gunji Y, Kurihara M, *et al.* Characteristics of pulmonary cysts in Birt–Hogg–Dubé syndrome: thin-section CT findings of the chest in 12 patients. *Eur J Radiol* 2011; 77: 403–409.

127 Gupta N, Kopras EJ, Henske EP, *et al.* spontaneous pneumothoraces in patients with Birt–Hogg–Dubé syndrome. *Ann Am Thorac Soc* 2017; 14: 706–713.

128 Daccord C, Cottin V, Prévot G, *et al.* Lung function in Birt–Hogg–Dubé syndrome: a retrospective analysis of 96 patients. *Orphanet J Rare Dis* 2020; 15: 120.

129 Uehara Y, Tanaka Y, Zhao S, *et al.* Insights into pulmonary phosphate homeostasis and osteoclastogenesis emerge from the study of pulmonary alveolar microlithiasis. *Nat Commun* 2023; 14: 1205.

130 Castellana G, Castellana G, Gentile M, *et al.* Pulmonary alveolar microlithiasis: review of the 1022 cases reported worldwide. *Eur Respir Rev* 2015; 24: 607–620.

131 Vavassori S, Chou J, Faletti LE, *et al.* Multisystem inflammation and susceptibility to viral infections in human ZNFX1 deficiency. *J Allergy Clin Immunol* 2021; 148: 381–393.

132 Alder JK, Sutton RM, Iasella CJ, *et al.* Lung transplantation for idiopathic pulmonary fibrosis enriches for individuals with telomere-mediated disease. *J Heart Lung Transplant* 2021; 41: 654–663.

133 Zhang D, Povysil G, Kobeissy PH, *et al.* Rare and common variants in *KIF15* contribute to genetic risk of idiopathic pulmonary fibrosis. *Am J Respir Crit Care Med* 2022; 206: 56–69.